World Electric Vehicle Journal

MDPI

Article

Efficient Drone Data Collection in WSNs: ILP and mTSP Integration with Quality Assessment †

Gregory Gasteratos *,‡ **and Ioannis Karydis** ‡

Department of Informatics, Ionian University, 49132 Kerkyra, Greece; karydis@ionio.gr

* Correspondence: ggasteratos@ionio.gr

† This paper is an extended version of our paper published in the 3rd Asia-Europe Conference on Applied Information Technology (AETECH 2025) titled "Optimized Drone Data Collection in WSNs: An ILP and mTSP Framework".

‡ These authors contributed equally to this work.

Abstract

The proliferation of wireless sensor networks in remote and inaccessible areas demands efficient data collection approaches that minimize energy consumption while ensuring comprehensive coverage. Traditional data retrieval methods face significant challenges when sensors are sparsely distributed across extensive areas, particularly in scenarios where direct sensor access is impractical due to terrain constraints or operational limitations. This research addresses these challenges through a novel hybrid optimization framework that combines integer linear programming (ILP) with multiple traveling salesperson problem (mTSP) algorithms for drone-based data collection in wireless sensor networks (WSNs). The methodology employs a two-phase approach, where ILP optimally determines strategic access point locations for sensor clustering based on communication capabilities, followed by mTSP optimization to generate efficient inter-AP flight trajectories rather than individual sensor visits. Comprehensive simulations across diverse network configurations and drone quantities demonstrate consistent performance improvements, with travel distance reductions reaching 32% compared to conventional mTSP implementations. Comparative evaluation against established clustering algorithms including Voronoi, DBSCAN, Constrained K-Means, Graph-Based clustering, and Greedy Circle Packing confirms that ILP consistently achieves optimal access point allocation while maintaining superior routing efficiency. Additionally, a novel quality assessment metric quantifies sensor grouping effectiveness, revealing that ILP-based clustering advantages become increasingly pronounced with higher sensor densities, providing substantial operational benefits for large-scale wireless sensor network deployments.

Keywords: path planning optimization; drone path planning; ILP; mTSP; access points

Academic Editor: Michael Fowler

Received: 8 August 2025
Revised: 26 September 2025
Accepted: 28 September 2025
Published: 1 October 2025

Citation: Gasteratos, G.; Karydis, I. Efficient Drone Data Collection in WSNs: ILP and mTSP Integration with Quality Assessment. *World Electr. Veh. J.* **2025**, *16*, 560. https://doi.org/10.3390/wevj16100560

1. Introduction

Gathering data effectively from extensive networks of sensors presents a significant challenge, especially in places where setting up conventional systems is just not feasible. Wireless sensor networks (WSNs) [1] are being used more and more in diverse fields like environmental monitoring [2], precision agriculture [3], and disaster response [4]. A core difficulty in these setups is extracting the data efficiently, particularly when the sensors themselves cannot move around, have limited communication reach, and run on tight power resources. As highlighted by Balbal et al. [5], smart ways of collecting data can really make a difference in how well the whole network performs.

Unmanned Aerial Vehicles (UAVs) or drones have emerged as a promising solution for data collection in WSNs, particularly in large, sparsely populated areas. However, optimizing both the locations for data collection, known as access points (APs), and the routing of multiple drones presents significant challenges that existing approaches have not adequately addressed.

Recent research efforts have explored various optimization strategies for UAV-assisted data collection, yet critical methodological gaps remain. Bilevel optimization approaches, such as those employing improved dandelion algorithms combined with single Traveling Salesman Problem (TSP) [6] formulations, rely on heuristic methods that cannot guarantee optimal solutions for multi-drone scenarios [7]. Similarly, energy-efficient clustering strategies developed for traditional WSN applications focus primarily on ground-based energy distribution without considering the unique constraints of aerial data collection, including communication range limitations, drone energy consumption patterns, and multi-agent coordination requirements [8,9]. Specialized applications such as landslide monitoring with drone-assisted WSNs demonstrate domain-specific solutions but lack the generalized optimization framework needed for diverse deployment scenarios [10]. While these approaches demonstrate effectiveness in their specific domains, none combine the mathematical optimality guarantees of integer linear programming for strategic access point placement with the multi-agent efficiency of mTSP formulation for coordinated drone routing.

This paper extends our previous work [11] by exploring the deployment of multiple UAVs for data collection tasks using a hybrid approach that combines integer linear programming (ILP) [12] and the multiple Traveling Salesman Problem (mTSP) [13,14]. Building upon the foundational two-phase optimization strategy, this extended version introduces a comprehensive quality assessment framework for evaluating access point configurations and their operational impact on data collection efficiency. The aim is to minimize total energy consumption across all UAVs while ensuring complete sensor node coverage and optimal operational effectiveness.

Motivation and Contribution

The integration of unmanned aerial vehicles for the collection of data from ground sensors is a rapidly evolving field, particularly with respect to operational efficiency and resource optimization. The challenges of aerial data collection require innovative approaches that can address both coverage and routing problems simultaneously.

To this end, the contributions of this work can be summarized as follows:

- A Novel Two-Phase Optimization Framework. This work introduces a novel two-phase optimization framework to address the sensor data collection problem. The first phase uses an Integer Linear Program (ILP) to determine the minimum number of access points needed to cover all sensors, which significantly reduces the complexity of the subsequent routing problem. The second phase models the routing as a Multi-Traveling Salesman Problem (mTSP) to efficiently plan the drone paths to visit these access points, rather than individual sensors, minimizing overall travel distance.
- Operational Impact Assessment. The research develops a comprehensive quality assessment framework to evaluate the effectiveness of generated access point configurations. This framework uses metrics like compactness, maximum distance, and consistency to analyze operational impact, including predicted hover times and communication efficiency. Additionally, the work introduces a post-processing technique to refine the sensor-to-access point assignments, which further improves operational effectiveness while maintaining the minimal number of access points achieved in the initial ILP phase.

- Extensive Experimental Validation. The study performs extensive experimental validation to demonstrate the effectiveness of the proposed approach. The research conducts a comparative analysis against six established clustering algorithms including Voronoi tessellation, DBSCAN, Constrained K-Means, Graph-Based clustering, and Greedy Circle Packing, where the ILP consistently achieves the optimal access point minimization. Furthermore, simulated experiments across various network configurations and drone counts demonstrate significant performance advantages, with travel distance reductions of up to 32% compared to direct sensor visitation methods.

This approach not only minimizes the number of APs required but also optimizes drone paths, leading to significant improvements in energy efficiency and scalability. The primary benefit of separating the problem into two phases is the reduction in computational complexity. The combined problem of determining optimal AP locations and drone paths simultaneously would be NP-hard and practically unsolvable for large networks.

The ILP approach first identifies the minimum number of access point locations needed to provide complete sensor coverage, effectively grouping sensors into clusters around these optimal positions. This reduces the subsequent mTSP problem complexity since drones only need to visit APs rather than all individual sensors.

The remainder of this paper unfolds as follows. Section 2 examines relevant contributions, covering the foundational work of mTSP formulations and ILP techniques, alongside recent developments in hybrid approaches that merge clustering mechanisms with mobile collection strategies. Section 3 elaborates on our proposed methodology, detailing the two-phase optimization process where ILP determines optimal access point placement followed by mTSP route planning. Section 4 encompasses our experimental methodology, describing the test environment, presenting the various network configurations examined, and analyzing the performance outcomes through comparative distance metrics, clustering efficiency indicators, and comprehensive quality assessment frameworks. This section also introduces our post-processing enhancement technique and provides extensive comparative analysis against established clustering algorithms including Voronoi tessellation, DBSCAN, and Graph-Based approaches. The paper concludes in Section 5 with a synthesis of our findings and suggestions for extending this research in emerging Internet of Things (IoT) [15] contexts.

2. Background and Related Work

2.1. WSN Data Collection Approaches

Research in WSN data collection has evolved significantly over the past two decades [16], following several distinct but interconnected paths focusing on mobile collection, clustering approaches, and integrated methodologies.

2.1.1. Mobile Data Collectors (MDCs)

The concept of mobile elements for WSN data collection emerged in 2003 when Shah et al. introduced "Data MULEs" [17]. This seminal work established a new paradigm for employing mobile nodes to gather information from stationary sensors, addressing the power constraints inherent in long-range transmissions.

Several researchers subsequently expanded this foundational work. Gatzianas and Georgiadis [18] developed sophisticated linear programming models for resource allocation in WSNs with mobile access points. Their work emphasized network lifespan maximization while accounting for collector movement patterns. Chakrabarti et al. [19] investigated fundamental trade-offs between energy consumption and data latency in mobile collection scenarios. Their study established practical boundaries that continue to influence system

architecture decisions. These pioneering efforts collectively shaped our understanding of mobile data collection in wireless sensor environments.

Recent work has also explored bilevel optimization frameworks for UAV-assisted data collection. Han et al. [7] proposed a bilevel optimization approach where an improved dandelion algorithm optimizes UAV deployment at the upper level, while an iterated greedy algorithm addresses single TSP at the lower level. While this approach demonstrates effectiveness for single-UAV scenarios, it relies on heuristic methods that lack mathematical optimality guarantees and does not address the multi-drone coordination requirements inherent in large-scale WSN deployments. Later work by the same research group extended this to multi-UAV scenarios for large-scale mobile edge computing applications [20], though still relying on approximation algorithms rather than optimal solutions for the access point placement phase.

Specialized applications have also demonstrated the effectiveness of UAV-assisted data collection in specific domains. Karunanithy et al. [10] developed an energy-efficient data routing protocol specifically for landslide-prone areas, employing drones to collect data while minimizing human risk in hazardous environments. Their approach, while effective for disaster monitoring scenarios, focuses on reliability and safety rather than the general optimization of access point placement and routing efficiency.

Our ILP-based approach fundamentally differs by providing mathematical optimality for the critical access point placement phase while seamlessly integrating with mTSP for multi-drone coordination, offering a generalized framework that can adapt to diverse deployment scenarios.

2.1.2. AP/Cluster Head Selection

The selection of optimal cluster heads or access points in wireless sensor networks remains a crucial research challenge that has attracted considerable attention. In [21], Heinzelman et al. developed the LEACH (Low-Energy Adaptive Clustering Hierarchy) protocol, now recognized as a pioneering and influential protocol for WSN clustering. The innovation of LEACH lies in its approach to spreading energy consumption across the network through periodic rotation of cluster head responsibilities among nodes.

Building on the LEACH foundation, Younis and Fahmy [22] introduced HEED (Hybrid Energy-Efficient Distributed clustering), which advanced the clustering methodology by incorporating both remaining energy levels and communication costs as determining factors in the cluster head selection process. This strategy notably extended network operational time compared to previous methods. Gupta and Younis [23] specifically tackled the difficult issue of fault-tolerant clustering, developing techniques to bounce back from cluster head failures and sustain network connections despite losing nodes.

Recent advances in energy-efficient clustering have further developed these foundational approaches. Balanced energy-efficient clustering strategies have focused on optimizing energy distribution among ground-based sensor nodes through sophisticated load balancing mechanisms [9]. Advanced methods such as machine learning-based clustering protocols have demonstrated improved energy efficiency by integrating fuzzy c-means algorithms with optimized routing strategies for IoT-enabled WSN environments [8].

However, these methods are designed for traditional multi-hop routing scenarios and do not consider the unique constraints of aerial data collection, such as communication range limitations, drone energy consumption patterns, and flight trajectory optimization. While these clustering strategies excel in their intended ground-based applications, they lack integration with aerial vehicle coordination and multi-drone routing optimization that our approach provides.

2.1.3. Combined Approaches

Various researchers have investigated methods combining clustering elements with mobile collection, resembling the two-phase strategy under examination. One of the main differences between our method and previous approaches lies in how APs are conceptualized and used. Typically, related work treats APs—or cluster heads—as logical nodes within the network that gather sensor data and forward it using multi-hop communication, without the need for physical access. Our approach, however, takes a different route by treating APs as real-world locations that drones must physically visit. This redefinition turns APs from passive communication hubs into active data collection points, directly tying their placement to the drone's travel route. This role of APs—as both clustering anchors and compulsory drone checkpoints—marks a significant shift from established practices and is central to the performance gains demonstrated in our experiments. Gandham et al. [24] presented an early dual-stage approach employing ILP for determining base station locations followed by route enhancement. Their work demonstrated the benefits of breaking down complicated problems into more manageable components.

Roberti and Ruthmair [25] created a mixed-integer linear program (MILP) framework that synchronizes truck and drone logistics, leveraging the speed of drones alongside the capacity of trucks. Their methodology reflects a broader trend within the literature that recognizes the importance of co-deployment strategies involving different vehicle types, as it serves to optimize delivery processes in various operational settings. By aligning routing plans through ILP techniques [26], significant efficiency enhancements can be achieved, making it feasible for drones to cover greater distances with optimized energy usage.

Similarly, Meskar and Ahmadi [27] in their study integrated a realistic, load-dependent energy consumption function into a mixed-integer linear programming framework, allowing precise calculation of drone operational costs across various flight phases. By comparing different routing strategies and addressing demand uncertainty, the researchers therein provide a comprehensive method for determining optimal drone launching centers and delivery routes, demonstrating the significant advantages of an integrated approach over traditional sequential planning methods.

Moreover, the integration of advanced algorithms and computational techniques within the ILP framework can further enhance its applicability in dynamic environments. For instance, adaptive algorithms that adjust to changing environmental conditions can be developed to optimize AP placement and routing strategies in real-time [28].

2.1.4. Specific Work on ILP + mTSP for WSNs

Several research teams have examined the particular combination of ILP for selecting APs followed by mTSP for planning collection paths. Castaño et al. [29] put forward a comparable approach explicitly developed for urban monitoring using IoT devices.Their methodology employs ILP to determine the most effective gateway locations before addressing the mTSP for vehicles collecting data, demonstrating notable success in dense city environments.

Gu et al. [30] introduced a two-phase optimization solution for industrial WSNs, utilizing mixed-integer programming for relaying nodes' placement followed by route enhancements. Their research addressed the particular constraints found in industrial settings, including interference and reliability demands.

Cornejo-Acosta et al. [31] presented innovative methods for solving routing challenges across various mTSP variants by developing compact mathematical models with reduced computational complexity. Their proposal of integer programming formulations offers flexible solutions for real-world routing scenarios, demonstrating significant theoretical

and practical advantages in handling multiple salespersons' routes without traditional depot constraints.

2.2. Limitations of Existing Approaches

While existing research has made significant contributions to WSN data collection optimization, several critical shortcomings remain that directly motivate this work. Current approaches typically address access point placement or routing optimization in isolation but rarely both systematically, leading to suboptimal overall system performance.

Recent bilevel optimization methods, while representing advancement in UAV trajectory planning, suffer from fundamental limitations by relying entirely on heuristic algorithms at both optimization levels, providing no mathematical optimality guarantees for the critical access point placement phase. These approaches treat deployment and trajectory as separate optimization problems, missing opportunities for integrated optimization that our ILP + mTSP framework captures.

Similarly, advanced energy-efficient clustering strategies focus primarily on ground-based energy distribution without considering aerial collection constraints. Even sophisticated machine learning-based clustering protocols optimize for traditional multi-hop routing scenarios but fail to account for the communication range limitations, drone energy consumption patterns, and flight trajectory requirements inherent in UAV-assisted data collection.

Traditional clustering algorithms often produce suboptimal access point configurations, either generating excessive numbers of cluster heads that reduce routing efficiency or creating poorly distributed clusters that increase communication overhead and hover times for data collection drones. Moreover, existing methodologies lack comprehensive quality metrics that evaluate the operational efficiency of access point configurations, with most approaches focusing solely on coverage constraints without considering the practical implications of sensor distribution patterns within each cluster on drone energy consumption and collection times.

A fundamental gap exists between theoretical approaches and operational realities, as previous work treats access points as logical communication hubs rather than physical locations that drones must visit. This abstraction overlooks the critical relationship between cluster geometry and actual data collection efficiency, particularly how sensor dispersion within coverage areas affects communication quality and required hover times. Additionally, while some hybrid approaches show promise in small-scale scenarios, they fail to demonstrate consistent performance advantages as network size increases, limiting their applicability to large-scale environmental monitoring or precision agriculture deployments where the benefits of optimization become most critical.

These limitations highlight the need for a systematic two-phase approach that guarantees optimal access point minimization through ILP while providing comprehensive quality assessment frameworks to evaluate real-world operational efficiency. The proposed methodology addresses these gaps by integrating mathematical optimality with practical operational considerations, providing both theoretical guarantees and measurable performance improvements for drone-based WSN data collection systems.

2.3. Benefits of Using Integer Linear Programming

ILP is particularly effective for problems involving discrete variables, such as the placement of APs. Its primary benefit is yielding optimal solutions for complex combinatorial problems [32]. By formulating AP placement as an ILP, each sensor can be covered by exactly one AP while minimizing the total number of APs used [32].

ILP allows for the exploration of multiple objectives, such as minimizing the number of APs while maximizing coverage and connectivity. This multi-objective optimization is particularly relevant in scenarios where environmental conditions may vary, necessitating adaptive deployment strategies [33]. The flexibility of ILP in accommodating different constraints and objectives makes it a powerful tool for network design and optimization [34,35].

The findings of Kara and Bektas [36] suggest that solving the mTSP directly using their ILP formulations is more efficient than transforming it into a standard TSP. Similarly, Wang et al. [37] provide a comprehensive framework for aerial data collection in large-scale wireless sensor networks, supporting the notion that effective AP placement leads to significant improvements in data collection efficiency.

As researchers continue to bridge ILP with drone routing complexities, it becomes evident that these methodologies present a promising avenue for enhancing logistical efficiencies across varied applications, from disaster relief to commercial deliveries. In summary, the integration of integer linear programming within the paradigms of access point placement and Multi-Traveling Salesman Problem analysis for drone routing reveals a powerful capability for enhancing operational efficiencies.

3. Proposed Method

As mentioned previously, herein a two-phase optimization strategy is proposed as depicted in Figure 1.

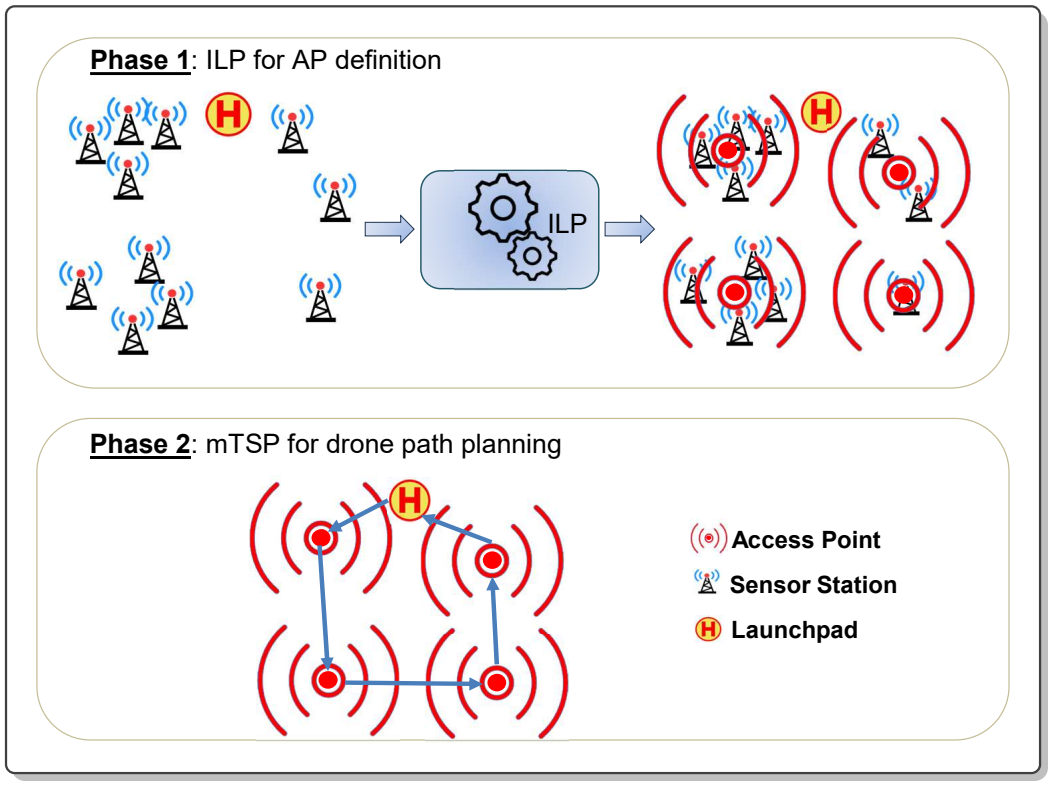

Figure 1. Two-phase optimization strategy.

3.1. Phase 1: ILP for APs' Placement

This phase entails the modeling of the access point placement challenge as an integer linear programming problem. This approach enables the efficient clustering of sensors based on their transmission capabilities.

To enhance the legibility of the work, an example scenario is employed for presentation purposes: as illustrated in Figure 2, the initial configuration of the scenario consists of 20 static sensor stations $(S_1 \ldots S_{20})$ distributed across a field. These stations continuously collect data that must be retrieved. At the designated launchpad (H), three drones are stationed for deployment to collect the data from the distributed sensors.

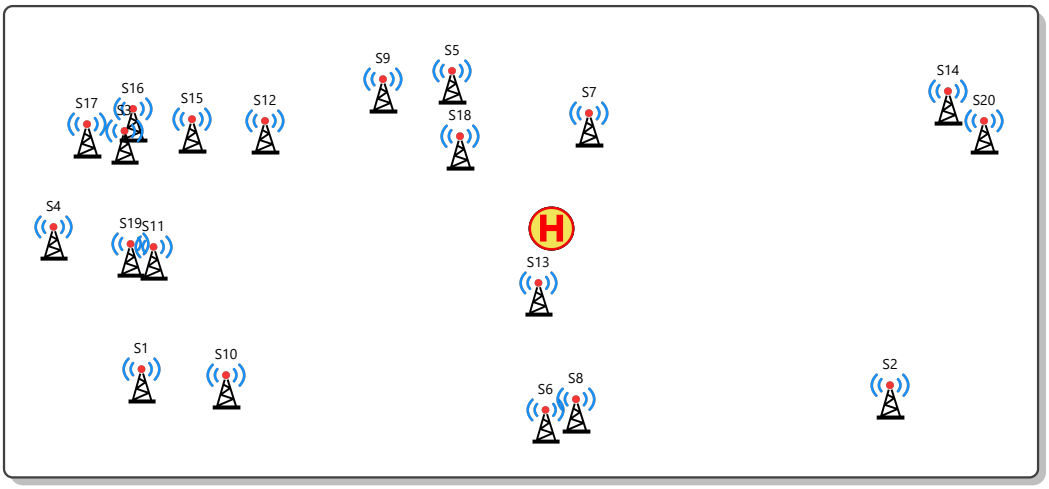

Figure 2. A random placement of sensor stations in a field.

By applying the ILP algorithm, stations have been grouped according to their data transmission range capabilities. The results of this optimization are depicted in Figure 3, where distinct clusters have been formed. These newly established groups, designated as access points, are clearly demarcated with circular boundaries in the illustration, wherein the center of the boundary is identified by the ILP and the radius is 100 units.

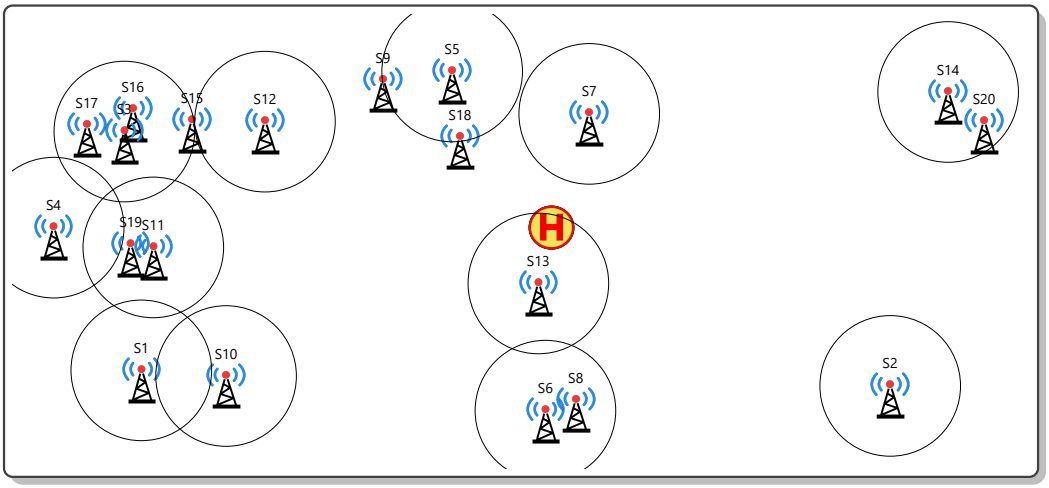

Figure 3. Application of ILP for APs' definitions.

These optimized access points now serve as consolidated collection locations, significantly streamlining the flight paths required for the drones to retrieve all sensors' data. Rather than visiting each individual sensor, the drones now need only to visit these strategically positioned access points.

The implementation of defining the APs using ILP is shown in Algorithm 1 where the GetAccessPointCoordinates is the name of the method returning the list of the AP locations.

Algorithm 1 GetAccessPointCoordinates.

Require: List of sensor coordinates $\mathcal{S} = \{(x_1, y_1), (x_2, y_2), \ldots, (x_n, y_n)\}$, coverage radius r
Ensure: List of selected access point coordinates $\mathcal{A}$ that minimize AP count while ensuring full sensor coverage

1: Initialize ILP solver using OR-Tools SCIP backend
2: Define candidate AP locations $\mathcal{C} \leftarrow \mathcal{S}$ ▷ Sensors can serve as potential AP locations
3: **Initialize decision variables:**
4: **for** $ap \in \mathcal{C}$ **do**
5: Define binary variable $isAP[ap] \in \{0, 1\}$ ▷ 1 if AP is placed at location ap, 0 otherwise
6: **end for**
7: **Initialize coverage variables:**
8: **for** $s \in \mathcal{S}$ **do**
9: **for** $ap \in \mathcal{C}$ **do**
10: **if** distance$(s, ap) \leq r$ **then** ▷ Check if sensor s is within coverage of AP ap
11: Define binary variable $covers[s, ap] \in \{0, 1\}$ ▷ 1 if AP ap covers sensor s, 0 otherwise
12: **end if**
13: **end for**
14: **end for**
15: **Add coverage constraints:** ▷ Each sensor must be covered by exactly one AP
16: **for** $s \in \mathcal{S}$ **do**
17: Add constraint: $\sum_{\text{ap such that } (s,ap) \in covers} covers[s, ap] = 1$
18: **end for**
19: **Add activation constraints:** ▷ If AP covers a sensor, that AP must be active
20: **for** $(s, ap) \in covers$ **do**
21: Add constraint: $covers[s, ap] \leq isAP[ap]$
22: **end for**
23: Set objective function: minimize $\sum_{ap \in \mathcal{C}} isAP[ap]$ ▷ Minimize total number of active APs
24: Solve ILP model
25: **Extract solution:**
26: $\mathcal{A} \leftarrow \emptyset$ ▷ Initialize empty result set
27: **if** solution status is OPTIMAL **then**
28: **for** $ap \in \mathcal{C}$ **do**
29: **if** $isAP[ap] = 1$ **then** ▷ If AP is selected in optimal solution
30: Add ap to $\mathcal{A}$ ▷ Include in final AP set
31: **end if**
32: **end for**
33: **else**
34: **return** INFEASIBLE or ERROR ▷ Handle cases where no solution exists
35: **end if**
36: **return** $\mathcal{A}$ ▷ Return optimal AP locations

The ILP formulation addresses the access point placement problem as a combinatorial optimization challenge with the following key components:

Decision Variables:

- $isAP[ap]$: Binary variable indicating whether an access point is placed at candidate location ap
- $covers[s, ap]$: Binary variable indicating whether access point ap provides coverage to sensor s

Constraints:

- *Coverage constraint*(line 16): Ensures each sensor is covered by exactly one access point, preventing both under-coverage and redundant coverage
- *Activation constraint*(line 20): Enforces that if an access point covers any sensor, that access point must be activated (selected in the solution)

Objective Function:The objective minimizes the total number of access points while satisfying all coverage requirements, achieving the optimal clustering solution that reduces subsequent drone routing complexity.

Computational Considerations:The ILP approach guarantees mathematical optimality for the access point placement phase, providing the foundation for efficient mTSP routing in Phase 2. The computational complexity is manageable for typical WSN deployment scenarios with hundreds of sensors.

Algorithm Output Validation:The algorithm returns the minimal set of access point locations that ensure complete sensor coverage. Each returned coordinate in set $\mathcal{A}$ represents an optimal access point location where drones will collect data from all sensors within the coverage radius r. The optimality guarantee distinguishes this approach from heuristic clustering methods that may produce suboptimal access point configurations.

3.2. Phase 2: mTSP for Drone Path Planning

The second phase leverages the mTSP methodology, applying it to the newly established access points $(AP_1 \ldots AP_{12})$ from Figure 3 rather than addressing each sensor individually. Each drone receives a specific mission assignment consisting of a predefined route with designated access points and their associated sensor identifications. Each drone is exclusively responsible for collecting data from sensors assigned to its designated access points, ensuring systematic coverage without overlap or interference. Even if a drone operates in proximity to sensors assigned to other drones' access points, it only collects data from sensors within its own mission parameters. This approach maintains operational clarity, prevents data collection conflicts, and ensures that each sensor's data is collected exactly once according to the optimized assignment.

With the same deployment plan as stated before, i.e., three drones, Figure 4 demonstrates the optimized results, with the drones covering a total distance of 4805 units. Drone 1 flies the orange route $(H, AP_{12}, AP_2, AP_6, AP_{11}, H)$ covering 1767 units. Drone 2 flies the blue route $(H, AP_9, AP_4, AP_1, AP_8, H)$ covering 1571 units, and drone 3 flies the green route $(H, AP_7, AP_5, AP_{10}, AP_3, H)$ covering 1467 units.

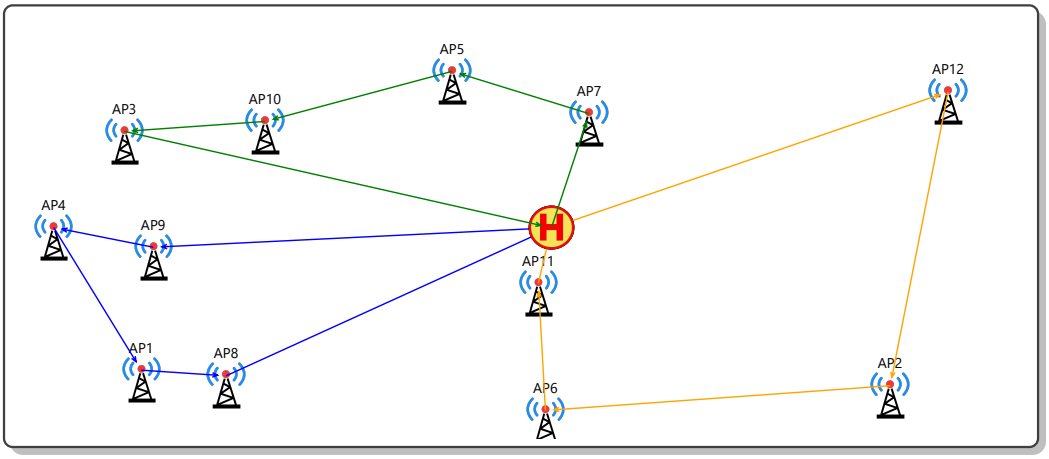

Figure 4. Apply mTSP on the APs. Different colored lines denote planned drone trajectories.

To evaluate the effectiveness of this strategic approach, a parallel analysis was conducted, applying mTSP directly to the original configuration illustrated in Figure 2, i.e., before the application of the ILP and the formation of the clusters/APs. Using identical parameters—the same number drones and identical launch location—Figure 5 displays these results, showing a total required travel distance of 5054 units. Drone 1 flies the orange route $(H, S_{13}, S_6, S_8, S_2, S_{20}, S_{14}, S_7, H)$ covering 1894 units. Drone 2 flies the blue

route $(H, S_{10}, S_1, S_4, S_{19}, S_{11}, S_9, S_5, H)$ covering 1770 units and drone 3 flies the green route $(H, S_{18}, S_{12}, S_{15}, S_{16}, S_{17}, S_3, H)$ covering 1390 units.

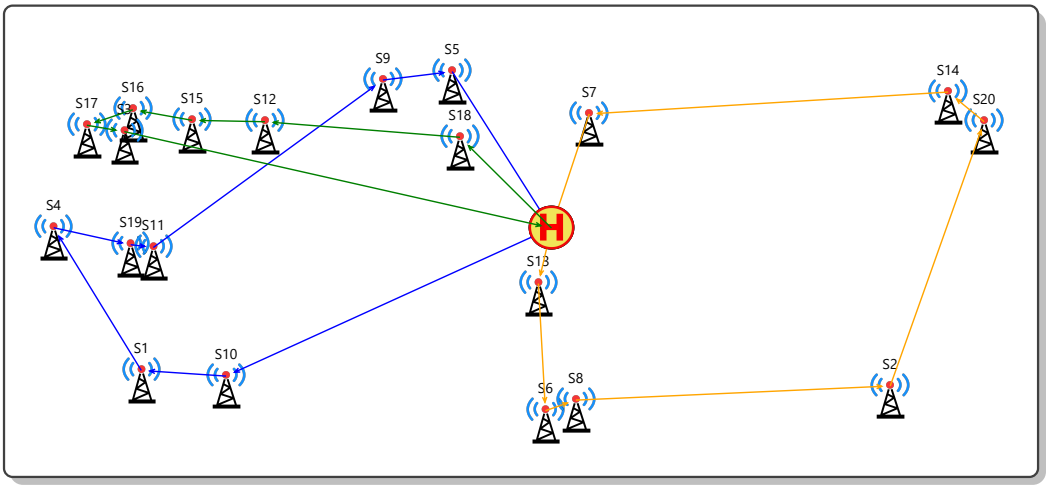

Figure 5. Application of mTSP on the stations without the use of ILP/APs. Different colored lines denote planned drone trajectories.

A comparative examination of both approaches reveals significant operational benefits. The optimized approach in Figure 4 requires navigation to only 12 collection points, whereas the conventional approach in Figure 5 necessitates visits to all 20 original locations. This strategic consolidation translates to considerable reduction on the required travel distance when implementing the access point methodology. This efficiency improvement on travel distance units demonstrates the tangible operational advantages of the clustered routing strategy through intermediate aggregation points.

3.3. Benefits of the Two-Phase Approach

After determining optimal AP locations through ILP in the first phase, the second phase uses the mTSP framework to optimize drone routing for data collection. This approach treats the previously determined APs as nodes in a graph, with drones functioning as multiple salesmen tasked with visiting these nodes. The objective is to reduce the overall journey length or duration while guaranteeing that each AP receives exactly one visit from exactly one drone.

By formulating the problem this way, efficient flight paths for multiple drones can be generated, balancing workload across the fleet while minimizing energy consumption.

This methodology scales well with network expansion. When new sensor stations are introduced, the number of required APs may not increase proportionally, particularly if these stations are positioned within the communication range of existing APs. The mTSP framework can readily accommodate additional APs as it will be shown in the experimentation section herein.

In addition, a significant advantage of this decoupled two-phase approach is its adaptability to dynamic field conditions. Modifications in station deployment or operational status can be addressed by reconfiguring APs' placements while maintaining existing drone paths where feasible. Conversely, changes in drone fleet composition or availability can be managed by adjusting routing solutions without necessitating alterations to the established AP infrastructure.

Finally, this sequential approach significantly reduces computational complexity compared to attempting to optimize both APs' placement and drone routing simultaneously.

3.4. Data Collection Efficiency at Access Points

The optimization benefits demonstrated thus far focus exclusively on inter-AP movement without considering the operational efficiency of data collection at each access point. This represents a significant analytical gap, as the time and energy required for hovering and data transmission can vary dramatically based on how stations are spatially distributed within the coverage area of each AP.

When a drone visits an individual station station directly, it hovers directly above the station with optimal signal strength and minimal communication time. However, when visiting an access point, the drone positions itself at the AP center and must communicate with all assigned stations within the coverage radius. Stations located near the coverage edge experience weaker signal strength, higher packet loss rates, and require longer transmission times compared to stations clustered near the AP center.

In other words, the distribution pattern of stations within each AP coverage area directly impacts operational efficiency. A drone requires significantly more time collecting data from an AP where stations are scattered across the coverage perimeter compared to one where stations cluster near the center position.

The proposed optimization herein, up to this point, addresses only the travel component while ignoring the potentially significant energy costs associated with hovering and communication phases. This observation highlights the necessity of developing metrics that evaluate AP quality based on station distribution characteristics and conduct further experiments.

3.4.1. Access Point Quality Metrics

The evaluation of access point data collection efficiency requires a comprehensive assessment framework that captures how sensor spatial distribution patterns affect operational performance. While the ILP optimization successfully minimizes access point count and ensures coverage, it does not account for the quality of sensor clustering within each coverage area, which directly impacts the communication efficiency and hover time requirements.

To address this gap, we develop a composite quality assessment methodology that integrates multiple geometric and operational characteristics into unified metrics. The mathematical framework utilizes the notation defined below defining all variables used in Equations (1) through (4).

Building upon the mathematical components defined in Table 1, a composite quality index is proposed, as defined in Equation (1), that integrates multiple geometric and operational characteristics into a unified assessment technique. The composite AP quality score combines three fundamental aspects of station distribution within each access point's coverage area:

$$Q_{AP} = \max\left(0, 1 - \left(w_1 \cdot Q_{compactness} + w_2 \cdot Q_{maxdist} + w_3 \cdot Q_{consistency}\right)\right) \quad (1)$$

where $w_1 = 0.4$, $w_2 = 0.3$, and $w_3 = 0.3$ represent the relative importance weights for each quality dimension. This formulation treats each component as a penalty factor, where higher component values indicate poorer AP configuration, and the overall quality score approaches 1.0 for optimal configurations. The parametric weighting approach enables adaptive reconfiguration for unforeseen scenarios where operational priorities or mission constraints deviate from standard assumptions.

Table 1. Mathematical notation for access point quality metrics.

Symbol	Type	Definition
Q_{AP}	Quality score	Composite Access Point quality score (0-1 range)
w_1, w_2, w_3	Weights	Relative importance weights (0.4, 0.3, 0.3)
$Q_{compactness}$	Component	Compactness penalty factor based on station clustering
$Q_{maxdist}$	Component	Maximum distance penalty factor
$Q_{consistency}$	Component	Consistency penalty factor based on distribution uniformity
$\sigma_{distance}$	Distance (meters)	Standard deviation of station distances from AP center
$r_{coverage}$	Distance (meters)	Coverage radius for access point
d_{max}	Distance (meters)	Maximum distance from AP center to any assigned station
c	Coordinate	Access Point center coordinate
s_i	Coordinate	Station i coordinate

Compactness Component

The compactness component $Q_{compactness}$, as defined in Equation (2), evaluates how efficiently stations utilize the available coverage area:

$$Q_{compactness} = \frac{\bar{d}}{r_{coverage}} \tag{2}$$

where $\bar{d}$ represents the average distance from the AP center to all assigned stations, and $r_{coverage}$ denotes the maximum coverage radius. Values approaching 0 indicate stations clustered near the AP center, enabling optimal communication efficiency, while values near 1.0 suggest stations distributed at the coverage perimeter, requiring maximum transmission power and extended collection times.

Maximum Distance Component

The maximum distance component $Q_{maxdist}$, as defined in Equation (3), captures the worst-case communication scenario within each AP:

$$Q_{maxdist} = \frac{d_{max}}{r_{coverage}} \tag{3}$$

where $d_{max} = \max_i(\|c - s_i\|)$ represents the maximum distance from AP center c to any assigned station s_i. Low values indicate all stations remain within close proximity to the AP center, while high values approaching 1.0 signal that some stations operate at the communication range limit, potentially requiring additional transmission attempts and extended hover times.

Consistency Component

The consistency component $Q_{consistency}$, as defined in Equation (4), quantifies the uniformity of sensor distribution around the AP center:

$$Q_{consistency} = \frac{\sigma_{distance}}{r_{coverage}} \tag{4}$$

where $\sigma_{distance}$ represents the standard deviation of distances from the AP center to assigned stations. Values near 0 indicate uniform station clustering with predictable communication

requirements, while higher values suggest irregular distribution patterns that complicate mission planning and introduce operational uncertainty. The normalization by coverage radius ensures consistency measures remain comparable across different AP configurations and deployment scenarios.

This composite metric combines all quality factors into a single score where values approaching 1.0 indicate optimal AP configurations for efficient data collection.

Table 2 summarizes how the quality score of an access point (AP) configuration affects the data collection efficiency and required hover time. Higher scores (closer to 1.0) indicate excellent performance with no additional hover time needed. As the score decreases, collection efficiency degrades, and additional hover time is required to compensate—ranging from 10 to 20% for good scores to over 40% for poor ones. APs with poor quality metrics may experience longer hover times compared to well-clustered configurations. In large networks where our method achieves the greatest travel distance reductions, this hovering penalty could offset some of the energy savings from optimized routing.

Table 2. Impact of quality score on collection efficiency and hover time.

Quality Score	Collection Efficiency	Hover Time Impact
0.8–1.0	Excellent	No extra time
0.6–0.8	Good	+10–20% hover time
0.4–0.6	Fair	+20–40% hover time
0.0–0.4	Poor	+40% + hover time

The weighted combination of these three components provides a comprehensive assessment of AP quality, with the compactness factor receiving the primary emphasis ($w_1 = 0.4$) due to its direct impact on communication efficiency, while the maximum distance and consistency factors contribute equally ($w_2 = w_3 = 0.3$) to capture the reliability and predictability aspects of data collection operations.

3.4.2. Operational Impact-Based Quality Assessment

Building upon the individual AP quality metrics described in the previous section, practical drone deployment scenarios require a more comprehensive evaluation technique that captures the real-world operational consequences of AP placement decisions. While the standard deviation distance, maximum distance, and compactness ratio provide valuable insights into station clustering characteristics, they do not directly translate into actionable information about mission duration, energy consumption, or operational reliability.

The operational impact-based approach shifts focus from geometric properties to mission-critical performance indicators. This methodology recognizes that drone operators primarily concern themselves with total mission time and operational predictability rather than abstract clustering metrics. The mathematical formulation employs the notation presented in Table 3 defining all variables used in Equations (5) through (10).

Using the mathematical components defined in Table 3, the assessment methodology quantifies how AP quality variations translate into tangible operational outcomes, such as extended hover times, increased communication overhead, and reduced mission reliability.

The operational assessment methodology evaluates each access point using a comprehensive technique that incorporates both quality-based time penalties and distance-dependent communication efficiency degradation. For access points exhibiting quality scores below the operational threshold $\tau_{good} = 0.8$, the system calculates additional hover time requirements using two complementary approaches. The quality-based penalty mechanism applies a linear relationship between quality degradation and time overhead,

while the distance-based penalty incorporates realistic communication physics to estimate retransmission and positioning requirements.

Table 3. Mathematical notation for operational impact assessment.

Symbol	Type	Definition
$t_{extra,i}$	Time (seconds)	Total operational extra time for access point i
$t_{quality,i}$	Time (seconds)	Quality-based time penalty for AP i
$t_{distance,i}$	Time (seconds)	Distance-based time penalty for AP i
τ_{good}	Threshold	Quality threshold for good performance (0.8) below which penalties are applied
q_i	Quality score	represents the normalized AP Quality Score for access point i (from Equation (1))
n_i	Integer	Number of stations assigned to access point i
$t_{station}$	Time (seconds)	Baseline optimal collection time per station (3 s)
$\eta_{comm,i}$	Efficiency factor	Communication efficiency factor for AP i (0.5–1.0)
η_{min}	Parameter	Minimum communication efficiency (0.5)
α	Parameter	Degradation rate parameter (1.5)
$d_{penalty,i}$	Penalty factor	Distance penalty for AP i (normalized, 0–1)
$d_{ratio,i}$	Ratio	Normalized average distance ratio for AP i
$\bar{d}_i$	Distance (meters)	Average distance from AP i to its assigned sensors
$d_{optimal}$	Threshold	Optimal distance ratio threshold (0.3)

The mathematical formulation for operational extra time calculation combines these factors as follows in Equation (5), taking the maximum to capture the dominant limiting factor:

$$t_{extra,i} = \max(t_{quality,i}, t_{distance,i}) \tag{5}$$

where the quality-based time penalty is expressed in Equation (6) as

$$t_{\text{quality},i} = \begin{cases} (\tau_{\text{good}} - q_i) \cdot n_i \cdot t_{\text{station}}, & \text{if } q_i < \tau_{\text{good}} \\ 0, & \text{otherwise} \end{cases} \tag{6}$$

where the variables are defined in Table 3: q_i represents the AP quality score (Q_{AP}) for AP i as calculated in Section 3.4.1 using Equation (1), n_i denotes the number of stations assigned to AP i, and $t_{station} = 3sec$ represents the baseline collection time per station under optimal conditions.

The distance-based penalty, as defined in Equation (7), incorporates communication efficiency degradation. This distance-based penalty accounts for communication degradation as sensors operate farther from their assigned access point center, requiring additional time for reliable data transmission:

$$t_{distance,i} = \frac{n_i \cdot t_{station}}{\eta_{comm,i}} - n_i \cdot t_{station} \tag{7}$$

The communication efficiency factor $\eta_{comm,i}$ (see Table 3) as defined in Equation (8) models real-world wireless signal degradation based on distance-dependent physics such as the average station distance within the coverage area:

$$\eta_{comm,i} = \max\left(\eta_{min}, 1 - (d_{penalty,i})^{\alpha}\right) \tag{8}$$

where $\eta_{min} = 0.5$ establishes the minimum communication efficiency, and $\alpha = 1.5$ controls the degradation rate. A non-linear degradation function is employed $(d_{penalty,i})^{\alpha}$ because real-world wireless communication exhibits non-linear distance-dependent behavior rather than simple linear degradation. Signal strength drops with distance squared according to the inverse square law [38], packet loss increases exponentially as signal weakens [39], and retransmission needs grow rapidly at communication limits [40]. The selection of $\alpha = 1.5$ represents a balance between mathematical realism and practical applicability expecting wireless communication to be fairly robust at moderate distances but to degrade more noticeably as sensors approach the limits of the coverage area, as $\alpha = 2$ (quadratic relationship) would create overly harsh efficiency drops that degrade too quickly with distance, while $\alpha = 1$ would produce unrealistic linear behavior that fails to capture the exponential nature of wireless communication degradation. $\alpha = 1.5$ provides moderate non-linear degradation that aligns with empirical wireless behavior observed in drone-sensor communication scenarios, offering a reasonable approximation of actual communication physics without excessive computational complexity. $1 - (d_{penalty,i})^{\alpha}$ converts penalty to efficiency (higher penalty = lower efficiency). $\max(\eta_{min}, \ldots)$ ensures minimum 50% efficiency (worst case).

The distance penalty $d_{penalty,i}$ (defined in Table 3) is calculated in Equation 9 as

$$d_{penalty,i} = \frac{d_{ratio,i} - d_{optimal}}{1 - d_{optimal}} \tag{9}$$

where $d_{ratio,i} = \frac{\bar{d}_i}{r_{coverage}}$ represents the normalized average distance for AP i, and $d_{optimal} = 0.3$ defines the optimal distance ratio (all variables defined in Table 3). This penalty quantifies how far beyond the optimal distance ratio the sensors are positioned, with values of 0 indicating optimal positioning and values approaching 1 representing maximum deviation.

The mathematical reasoning behind Equation (9) centers on creating a penalty system that appropriately scales sensor distribution effects on communication efficiency. The goal is to convert the distance ratio, which ranges from 0 to 1, into a distance penalty that equals 0 when the distance ratio is at or below $d_{optimal}$ (0.3, the optimal zone), equals 1 when the distance ratio reaches 1.0 (the coverage edge), and provides linear scaling between these critical points.

The transformation process involves two essential mathematical steps. First, the origin is shifted by subtracting 0.3 from the distance ratio ($d_{ratio,i} - d_{optimal}$), which repositions the coordinate system so that when the distance ratio equals 0.3, the penalty component becomes zero, and when the distance ratio equals 1.0, the penalty component becomes 0.7. Second, this shifted value is scaled to fit the 0–1 range by dividing by 0.7, which is calculated as $1 - d_{optimal}$ (1.0–0.3). This scaling ensures that when the penalty component equals zero, the final result is 0 divided by 0.7, which equals 0, and when the penalty component equals 0.7, the final result is 0.7 divided by 0.7, which equals 1. The specific values used in this formula reflect the concept of usable range within the coverage area. The total possible range spans from 0.0 to 1.0, representing the full coverage radius, while the optimal range extends from 0.0 to 0.3, representing the no-penalty zone where sensors operate with maximum communication efficiency. The penalty range covers 0.3 to 1.0,

which is where graduated penalties are applied based on distance from the access point center. The denominator value of 0.7, calculated as $1 - d_{optimal}$ (1.0–0.3), represents this penalty-applicable range, essentially the portion of the coverage area where communication efficiency begins to degrade and penalties become necessary.

Alternative approaches demonstrate why this specific formulation is necessary. A simple linear approach using just the distance ratio would incorrectly apply penalties even within the optimal zone from 0 to 0.3, while a simple shift subtracting 0.3 would produce negative values and fail to properly scale the results. Incorrect scaling approaches would maintain negative values and produce wrong scale ranges, failing to achieve the desired 0–1 penalty mapping that accurately reflects communication physics in drone-sensor scenarios.

This operational technique also identifies problematic access points that require special attention during mission planning as defined in Equation (10). Access points with quality scores $q_i < \tau_{prob}$ are flagged, as these locations typically experience significant communication challenges and extended collection times. The number of such problematic APs within a flight plan is quantified as

$$N_{\text{problematic}} = \sum_{i=1}^{N_{AP}} \begin{cases} 1 & \text{if } q_i < \tau_{prob} \\ 0 & \text{otherwise} \end{cases} \tag{10}$$

where N_{AP} denotes the total number of access points in the flight plan and τ_{prob} is a problematic quality threshold of 0.5 based on the values of Table 2. This counts how many access points have quality scores below the problematic threshold, which is used as a metric for assessing the reliability and operational risk of the flight plan.

3.4.3. Composite Quality Index

While operational impact assessment provides crucial insights into individual AP performance, mission planners require a unified metric that synthesizes multiple quality dimensions into a single interpretable score. The complexity of modern drone operations involves balancing numerous competing factors, including average performance, worst-case scenarios, operational consistency, time efficiency, and system reliability. Individual metrics, while valuable for detailed analysis, prove insufficient for holistic flight plan evaluation and comparative assessment between alternative routing strategies.

The proposed composite quality index addresses this limitation by integrating five distinct performance dimensions through a weighted aggregation technique. To simplify the mathematical notation, let Q denote the composite quality score, and Q_1 through Q_5 represent the individual quality components as defined in Table 4.

Each component captures a specific aspect of flight plan quality, with weights assigned based on operational priority and impact on mission success. The mathematical formulation, as defined in Equation (11), combines these factors as

$$Q = \sum_{i=1}^{5} w_i \cdot Q_i \tag{11}$$

The average quality component Q_1 represents the arithmetic mean of individual AP quality scores across the entire flight plan, providing insight into overall system performance. This metric captures the baseline operational efficiency expected during normal mission execution.

The worst-case quality component Q_2 corresponds to the minimum quality score encountered within the flight plan, highlighting potential operational bottlenecks. This factor ensures that composite scores reflect the practical reality that mission performance often depends on the weakest system component rather than average performance.

Table 4. Mathematical notation for composite quality index defining all variables used in Equations (11) through (14).

Symbol	Type	Definition
Q	Quality score	Unified composite quality metric (0–1 range)
w_1, w_2, w_3, w_4, w_5	Weights	Component importance weights (0.3, 0.2, 0.2, 0.2, 0.1)
Q_1	Component	Average quality: arithmetic mean of individual AP quality scores
Q_2	Component	Worst-case quality: minimum quality score in flight plan
Q_3	Component	Consistency: quality variation based on standard deviation
Q_4	Component	Time efficiency: ratio of baseline to actual collection times
Q_5	Component	Reliability: assessment based on problematic AP detection
$\sigma_{quality}$	Statistical measure	Standard deviation of AP quality scores across flight plan
$T_{baseline}$	Time (seconds)	Optimal collection time under ideal conditions
T_{extra}	Time (seconds)	Additional time requirements due to quality degradation
$N_{problematic}$	Integer count	Number of APs with quality scores below τ_{prob}
N_{AP}	Integer count	Total number of Access Points in flight plan
τ_{prob}	Threshold	Problematic quality threshold (0.5)

The consistency component Q_3, as defined in Equation (12), quantifies quality variation across APs using standard deviation-based measures:

$$Q_3 = 1 - \min(1, \sigma_{quality}) \tag{12}$$

where $\sigma_{quality}$ represents the standard deviation of AP quality scores. High consistency indicates predictable operational conditions with $\sigma_{quality}$ approaching zero, while significant variation suggests uneven performance characteristics that complicate mission planning and execution. The standard deviation provides an intuitive measure of quality spread, expressed in the same units as the quality scores themselves.

The time efficiency component Q_4, as defined in Equation (13), evaluates the relationship between baseline collection time and quality-induced delays:

$$Q_4 = \frac{T_{baseline}}{T_{baseline} + T_{extra}} \tag{13}$$

where $T_{baseline}$ represents the optimal collection time under ideal conditions and T_{extra} quantifies additional time requirements due to quality degradation.

The reliability component Q_5, as defined in Equation (14), provides assessment based on problematic AP detection:

$$Q_5 = e^{-2 \cdot \frac{N_{problematic}}{N_{AP}}} \tag{14}$$

where $N_{problematic}$ denotes problematic APs as defined in Equation (10) and N_{AP} denotes the total number of access points in the flight plan. The -2 in the exponential function $e^{-2 \cdot ratio}$ is the decay rate that controls how quickly reliability drops as problematic APs increase. To determine the optimal exponent coefficient, analysis of how different values affect the reliability scoring across varying scenarios of problematic access point proportions reveals the impact of this parameter on assessment accuracy as depicted in Table 5.

Table 5. Effect of different exponent coefficients on reliability assessment.

Problematic %	$e^{-1 \cdot ratio}$	$e^{-2 \cdot ratio}$	$e^{-3 \cdot ratio}$	**Linear max**$(0, 1 - ratio)$
0%	1.00	1.00	1.00	1.00
10%	0.90	0.82	0.74	0.90
25%	0.78	0.61	0.47	0.75
50%	0.61	0.37	0.22	0.50
75%	0.47	0.22	0.11	0.25
100%	0.37	0.14	0.05	0.00

A decay rate of -1 produces penalties that are too gentle, maintaining 90% reliability even when 10% of access points are problematic, which may not adequately reflect the operational risk. Conversely, a decay rate of -3 creates excessively harsh penalties, dropping reliability to 74% with only 10% problematic access points, which could be unnecessarily conservative for most operational scenarios.

The value of -2 provides realistic operational impact modeling by producing reliability scores of 82% with 10% problematic access points, 61% with 25% problematic access points, and 37% with 50% problematic access points. These values align well with practical expectations about how flight plan reliability should degrade as the proportion of problematic access points increases.

The selection of the exponential approach with the exponent set to -2 reflects the balance needed for standard operational contexts where reliability assessment should be neither overly optimistic nor unnecessarily pessimistic. This decay rate ensures that small numbers of problematic access points receive proportionate penalties without completely undermining confidence in the flight plan, while still appropriately reflecting the increased operational risk associated with higher proportions of problematic access points.

The weighting scheme prioritizes average quality ($w_1 = 0.3$) as the primary performance indicator, followed by time efficiency ($w_4 = 0.2$) and worst-case performance ($w_2 = 0.2$) as secondary factors. Consistency ($w_3 = 0.2$) and reliability ($w_5 = 0.1$) provide additional nuance to the composite assessment while maintaining focus on operational outcomes.

This composite technique enables direct comparison between alternative flight plans and provides mission planners with a unified metric for evaluating overall operational effectiveness. The resulting scores range from 0 to 1 (Table 6), with higher values indicating superior operational characteristics and improved mission efficiency. By consolidating multiple performance dimensions into a single interpretable value, the composite quality index facilitates the systematic evaluation of different access point configurations and routing strategies, allowing operators to make informed decisions about flight plan selection based on comprehensive quality assessment rather than individual metric optimization.

Table 6. Impact of composite score on flight plan quality and collection time.

Composite Score	Flight Plan Quality	Expected Impact
0.8–1.0	Excellent	Minimal extra time
0.6–0.8	Good	+10–20% collection time
0.4–0.6	Fair	+20–40% collection time
0.2–0.4	Poor	+40% + collection time
0.0–0.2	Very Poor	Significant delays

3.4.4. Quality-Based Post-Processing Enhancement

While the composite quality index provides a comprehensive technique for evaluating flight plan effectiveness, the practical application of ILP-based access point placement reveals inherent limitations that can significantly impact operational efficiency. To demonstrate these challenges and their resolution, an examination of the example configuration presented in Figure 6 is conducted, which illustrates an 11-station deployment scenario processed through our two-phase optimization approach.

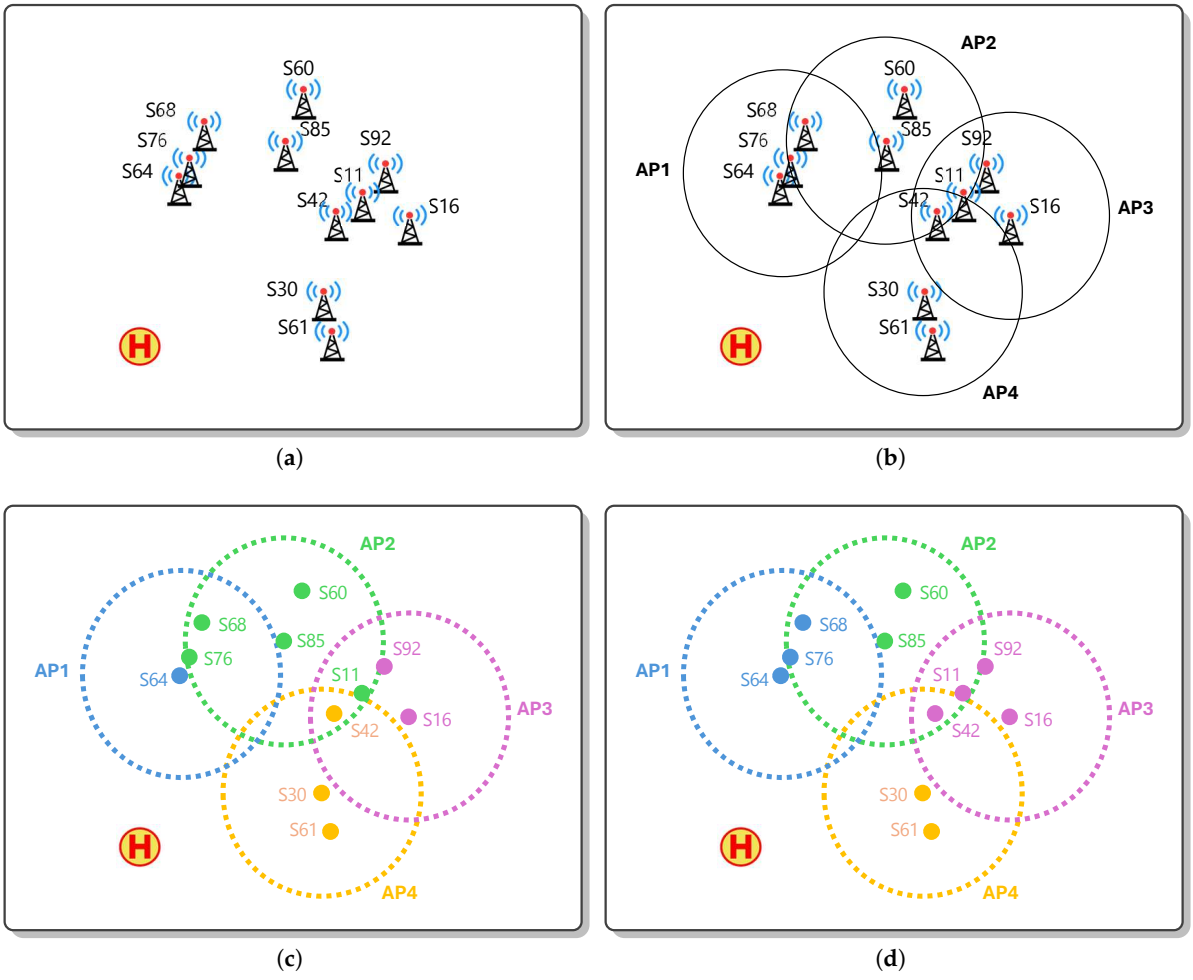

Figure 6. Enhancing station selection for APs. (**a**) 11 sensor stations in a field. (**b**) Applying ILP on (**a**) for AP placement. (**c**) Same as (**b**) to show clearly the station allocation in each AP. (**d**) Enhanced station selection for each AP.

Figure 6a presents the initial distribution of 11 sensor stations across the operational area. Following ILP optimization for access point placement, Figure 6b displays the resulting four access points with their associated coverage areas. Figure 6c reproduces the

same configuration using color coding to clearly delineate the access point assignments and their respective station allocations. Upon closer examination of this ILP-generated solution in Figure 6d, a critical operational challenge becomes apparent regarding station-to-access-point assignments.

The ILP formulation, while successfully minimizing the total number of access points, does not guarantee optimal station-to-AP assignments from a communication efficiency perspective. Stations may be assigned to access points that satisfy coverage constraints but are not necessarily the nearest available option. This phenomenon occurs because the ILP objective function prioritizes minimizing access point count over optimizing individual station assignment distances. Consequently, some stations operate closer to the communication range limits of their assigned access points rather than benefiting from proximity to potentially closer alternatives.

Applying the quality assessment (Equation (11)) to the ILP-generated configuration reveals the operational impact of these suboptimal assignments (Figure 6c, Table 7). The analysis yields a composite quality score of 0.62, indicating fair operational performance with room for significant improvement. More critically, the predicted extra hover time reaches 11.66 s, representing substantial operational overhead that directly impacts mission efficiency and energy consumption.

Table 7. Access point quality and associated stations for Figure 6c.

Access Point	Quality	Station(X, Y)
AP1	1	S64(299, 133)
AP2	0.35	S11(479, 151), S60(419, 51), S68(320, 83), S76(306, 117), S85(400, 101)
AP3	0.64	S16(524, 175), S92(500, 125)
AP4	0.51	S30(438, 248), S42(450, 171), S61(447, 286)

The detailed access point analysis exposes considerable quality variation across the four AP locations. AP1 achieves perfect quality (1.00) due to its single assigned station, while AP2 demonstrates poor performance (0.35) resulting from four stations distributed across varying distances from the access point center. AP3 and AP4 exhibit moderate quality scores of 0.64 and 0.51, respectively, indicating mixed operational characteristics that contribute to the overall system inefficiency.

This quality degradation stems directly from the ILP constraint structure, which ensures coverage and minimizes access point count but does not incorporate distance optimization in station assignments. While the ILP solution successfully maintains the minimum number of access points required for complete coverage, the resulting station distribution patterns create communication challenges that translate into extended collection times and reduced operational efficiency.

To address this limitation, an approach is proposed that involves post-processing the ILP-generated access point locations to reassign stations to their nearest available access points while preserving the optimal access point count achieved through integer programming. Algorithm 2 implements this enhancement strategy by maintaining the ILP-determined access point positions but redistributing station assignments based on proximity criteria rather than the original ILP assignment constraints.

Algorithm 2 Assign sensor station locations to the nearest access point.

Require: List of station coordinates $S = \{s_1, s_2, \ldots, s_n\}$, list of access point centers $C = \{c_1, c_2, \ldots, c_k\}$, coverage radius r
Ensure: List of access points, each with a center and its assigned stations
Initialize empty map $\mathcal{M} \leftarrow \emptyset$ ▷ center → access point
for all $c \in C$ **do**
  $\mathcal{M}[c] \leftarrow$ new access point with center c and radius r
end for
for all $s \in S$ **do**
  $N_s \leftarrow \{c \in C \mid \text{distance}(s, c) \leq r\}$ ▷ Valid centers within radius
  if $N_s \neq \emptyset$ **then**
    $c^* \leftarrow \arg\min_{c \in N_s} \text{distance}(s, c)$ ▷ Nearest center
    Add s to $\mathcal{M}[c^*]$
  end if
end for
$A \leftarrow$ list of access points in $\mathcal{M}$ **return** A

The post-processing algorithm iterates through all station locations, calculating distances to each available access point within communication range, and assigns each station to the nearest feasible option. This approach preserves the fundamental optimization achievement of minimizing access point count while improving the geometric distribution of stations around their respective collection points.

Reapplying the quality assessment metrics (Equation (11)) following Algorithm 2 post-processing demonstrates substantial operational improvements (Figure 6d, Table 8). The composite quality score increases from 0.62 to 0.76, representing a significant enhancement in overall flight plan effectiveness. More importantly, the predicted extra hover time decreases from 11.66 s to 5.77 s, achieving a 50% reduction in operational overhead through improved station-to-access-point assignments.

Table 8. Access point quality and associated stations for Figure 6d.

Access Point	Quality	Station(X, Y)
AP1	0.67	S64(299, 133), S68(320, 83), S76(306, 117)
AP2	0.65	S60(419, 51), S85(400, 101)
AP3	0.51	S11(479, 151), S16(524, 175), S42(450, 171), S92(500, 125)
AP4	0.75	S30(438, 248), S61(447, 286)

The redistributed access point analysis reveals more balanced quality characteristics across all four AP locations. AP1 maintains reasonable performance (0.67) with three well-distributed stations, while AP2 achieves similar effectiveness (0.65) with its two assigned stations. AP3 accommodates four stations with moderate quality (0.51), and AP4 demonstrates good performance (0.75) with its two assigned stations. This more uniform quality distribution contributes to improved operational predictability and reduced mission complexity.

The post-processing approach effectively addresses the limitation inherent in pure ILP formulations while maintaining the fundamental optimization objective of minimizing access point count. By decoupling the access point placement problem from the station assignment optimization, this two-stage approach achieves superior operational characteristics without compromising the mathematical guarantees provided by integer linear programming for coverage and access point minimization.

4. Experimental Evaluation

4.1. Setup

To model the access point selection as an ILP problem, the mTSP framework was adapted from our prior research [41,42], and Google OR-Tools [43] was leveraged to simplify the implementation of ILP-based solutions. The code was developed in C# using the .NET framework. All tests were conducted on a high-performance system with the following specifications: 512 GB of RAM, an AMD® Ryzen Threadripper Pro 5955WX (AMD, Santa Clara, CA, USA) processor (16 cores, 32 threads, 4.0 GHz base clock), and four NVIDIA RTX A5000 GA102GL GPUs (NVIDIA, Santa Clara, CA, USA).

A total of 80 distinct flight plans, each representing a different scenario, were generated. These scenarios explored a range of station densities, specifically 5, 10, 15, 20, 25, 45, 60, and 100 stations, while accommodating varying drone counts from 1 to 10. The stations were randomly created using a uniform random distribution. To mitigate potential statistical variations arising from randomized station locations, for each scenario, 10 copies were created using the same number of stations and drones but different station locations, producing 800 total scenarios (80 scenarios × 10 copies). The results were averaged for each scenario to ensure statistical reliability.

4.2. Evaluation Results

To assess the effectiveness of this approach, two key metrics were used:

- Performance Improvement: Let D_0 denote the original mTSP distance when visiting all stations directly, and D_{AP} denote the mTSP distance when using the access point approach. As defined in Equation (15), the performance improvement P measures the gains achieved (in percentage) by the two-phase method compared to using mTSP alone. More specifically, it represents the percentage reduction in the total distance that drones need to travel when using access points instead of visiting every station individually:

$$P = 1 - \frac{D_{AP}}{D_0} \tag{15}$$

- Sparsity Ratio: Let N_{AP} denote the number of access points and N_S denote the number of stations. As defined in Equation (16), the sparsity ratio S indicates how efficiently access points are distributed relative to the number of stations. A ratio near to 1 suggests one access point per station, while a lower ratio implies shared access points among multiple stations. Essentially it captures how "dense" or "sparse" the access point deployment is relative to the full set of stations:

$$S = \frac{N_{AP}}{N_S} \tag{16}$$

The results obtained from the tests, as depicted in Figure 7, demonstrate a clear trend that aligns well with the theoretical expectations described herein on the two-phase optimization approach involving ILP and mTSP.

4.2.1. Performance Analysis

The performance metric, in percentage, shows consistent improvement across all tested scenarios.

The performance advantage increases substantially with network size. For small networks with 5–25 stations, the improvement ranges from 3 to 7%. However, for larger networks with 45–100 stations, the improvement jumps significantly to 16–32%.

The most dramatic performance gain occurs in the largest tested network of 100 stations, where the two-phase approach reduces travel distance by nearly one-third (32%) compared to the direct mTSP approach.

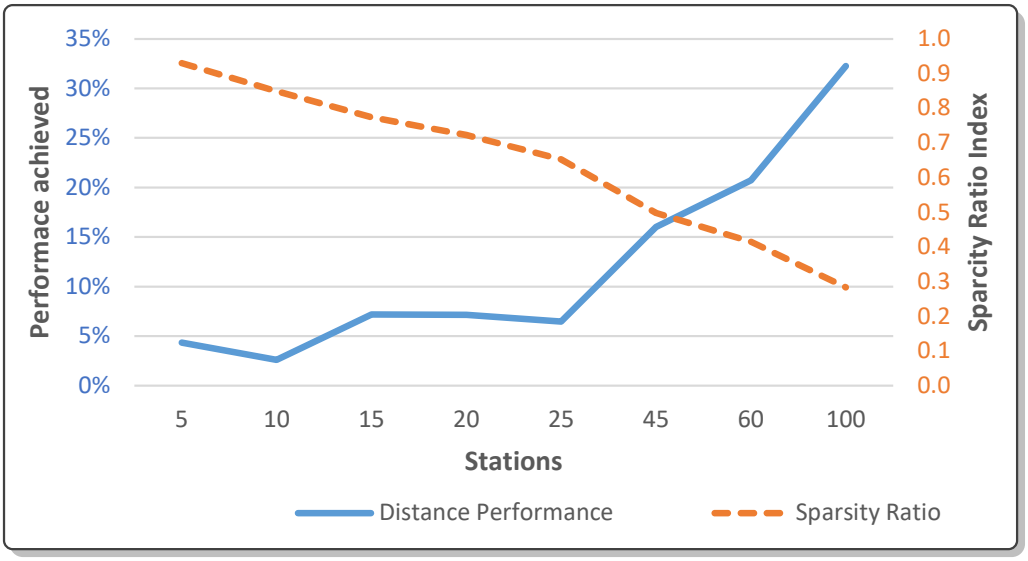

Figure 7. Distance performance by applying ILP for APs first and then mTSP.

4.2.2. Sparsity Analysis

The sparsity metric reveals important insights about the efficiency of the ILP phase. The sparsity decreases steadily as the number of stations increases, from 0.9 for 5 stations to 0.3 for 100 stations. This indicates that the clustering advantage becomes more pronounced in larger networks.

In small networks with 5 stations, nearly all stations serve as access points (sparsity = 0.9), offering minimal clustering benefit. However, in the largest network with 100 stations, only 30% of stations need to serve as access points.

The inverse relationship between sparsity and performance improvement confirms the paper's intuition: as more stations can be clustered under fewer access points, the efficiency gain of the two-phase approach increases.

4.2.3. Statistical Significance Analysis

To verify the statistical significance of the performance improvements, a Wilcoxon signed-rank test [44] is conducted across all 80 scenarios. The Wilcoxon test is selected as an appropriate non-parametric statistical method for this analysis because it does not assume normality in the data distribution, making it well-suited for comparing the paired observations of the two approaches (traditional mTSP versus our two-phase ILP + mTSP methodology).

The test yields a test statistic value of 3100.0 with a one-tailed p-value of 6.306×10^{-13} (N = 80). This extremely small p-value, orders of magnitude below the conventional threshold of 0.05, provides compelling evidence against the null hypothesis that the two approaches perform equally well. The magnitude of this result confirms that the distance reductions observed when implementing our two-phase optimization strategy represent genuine improvements rather than random variations.

The strength of this statistical evidence corresponds well with the pattern observed in Figure 7, where performance improvements become increasingly substantial as network complexity grows. The Wilcoxon test results validate our approach across the full spectrum of tested configurations, from small networks with minimal gains to large-scale deployments where the advantages become most pronounced.

This statistical confirmation is particularly valuable given the practical implications for drone battery life and operational efficiency in real-world applications. The significant *p*-value underscores the robustness of our approach and its potential value for implementation in various WSN data collection scenarios where resource optimization is critical.

4.2.4. Quality-Based Post-Processing Analysis

To validate the effectiveness of the quality-based post-processing enhancement (Section 3.4.4) across different network configurations, another experimental evaluation was conducted using the same testing framework described in Section 4.1. This systematic analysis (1600 additional tests) compares the composite quality scores (Equation (11)) achieved by the standard ILP approach against the enhanced ILP with post-processing assignment methodology across varying station densities ranging from 5 to 100 as shown in Figure 8.

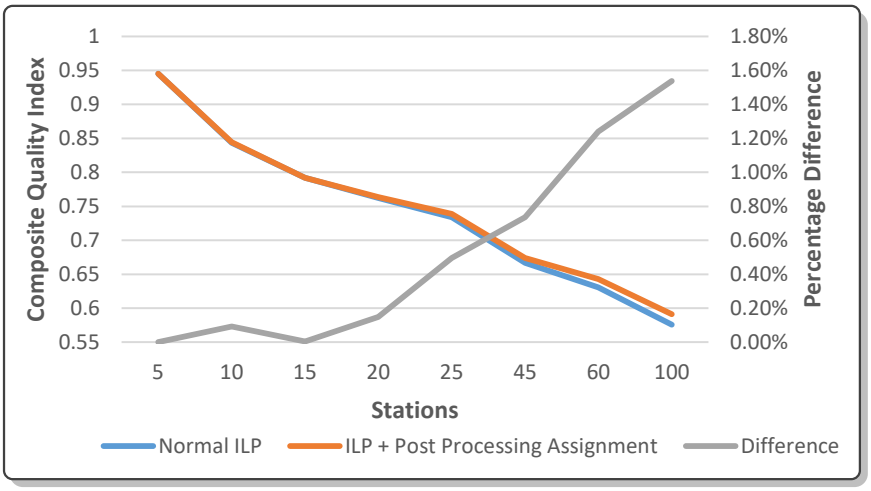

Figure 8. Composite quality scores by standard ILP approach against ILP with post-processing assignment to nearest AP center.

The comparative results demonstrate consistent improvements in composite quality scores when applying the post-processing assignment strategy. For smaller networks with five stations, both approaches achieve nearly identical performance, indicating that the ILP solution already produces near-optimal sensor assignments when the ratio of access points to stations is high, leaving minimal opportunity for post-processing improvements. However, as network complexity increases, the advantages of post-processing become increasingly pronounced. Medium-scale deployments with 25 to 45 stations show modest but consistent improvements. The most significant enhancements occur in large-scale networks where the original ILP approach demonstrates greater susceptibility to suboptimal station assignments. Networks with 100 stations exhibit quality improvements from 0.63 to 0.64, representing nearly a 2% enhancement in operational effectiveness through reassignment optimization alone.

4.3. Solidifying the Results

While the post-processing enhancement demonstrates modest improvements in operational quality, a comprehensive evaluation requires comparison against alternative clustering methodologies to validate the effectiveness of the ILP-based approach. The selection of access point placement algorithms fundamentally impacts both the number of collection points required and the resulting operational characteristics of drone-based data collection missions. To establish the relative merits of the proposed ILP methodol-

ogy, extensive comparative analysis was conducted against six established clustering and coverage algorithms commonly employed in wireless sensor network optimization.

The comparative study evaluates seven distinct approaches across identical experimental conditions.

- ILP provides mathematically optimal solutions by formulating access point placement as a constraint satisfaction problem that minimizes the number of coverage points while ensuring complete sensor coverage.
- Voronoi diagrams [45,46] creates natural clustering boundaries based on spatial proximity. It identifies which sensors are naturally grouped together based on their relative distances, then places access points to serve these spatially coherent clusters.
- Constrained K-Means [47,48] clustering adapts the traditional K-Means approach to incorporate coverage radius constraints, iteratively refining cluster centers to minimize within-cluster sensor distances while maintaining coverage requirements.
- DBSCAN (Density-Based Spatial Clustering of Applications with Noise) [49,50] identifies clusters based on sensor density patterns, automatically determining cluster boundaries and handling outlier sensors that may require individual access points.
- Graph-Based [51] clustering constructs connectivity graphs among sensors and applies graph partitioning algorithms to identify cohesive sensor groups, often producing high-quality clusters at the expense of additional access points.
- Greedy Circle Packing [52,53] algorithms employ iterative heuristics to place coverage circles, prioritizing areas with high sensor density and expanding coverage until all sensors are encompassed.

These methodologies represent fundamentally different approaches to spatial optimization, ranging from exact mathematical formulations to approximate heuristics designed for computational efficiency in large-scale deployments.

Using the experimental framework established in Section 4.1, 800 test scenarios were generated across varying sensor stations from 5 to 100, with identical hardware specifications and statistical averaging protocols being maintained for all algorithmic comparisons. To ensure fairness, all algorithms utilized the post-processing optimization technique detailed in Section 3.4.4. That resulted in 5600 additional test runs. This comprehensive evaluation examined four critical performance dimensions: access point count minimization, total flight distance optimization, mission time efficiency, and composite quality scores as developed in our quality assessment in Sections 3.4.1–3.4.3.

The results are presented in paired visualizations (Figures 9–12) where subfigure (a) displays the absolute performance values for each algorithm across varying network sizes, while subfigure (b) shows the percentage differences relative to ILP performance. This dual presentation approach was adopted to address the visual overlap inherent in comparing seven different algorithms simultaneously, ensuring that performance variations between methods remain clearly distinguishable across all tested scenarios. The percentage difference analysis in subfigure (b) facilitates direct quantitative comparison of each algorithm's efficiency relative to the ILP benchmark, with the X-axis representing ILP as the baseline reference point. Values plotted above the X-axis indicate that ILP outperforms the corresponding algorithm by the displayed percentage, while values below the X-axis would indicate superior performance by the alternative method. This visualization framework highlights both the magnitude and consistency of performance gaps across different network configurations, demonstrating the competitive advantage of ILP across multiple operational dimensions.

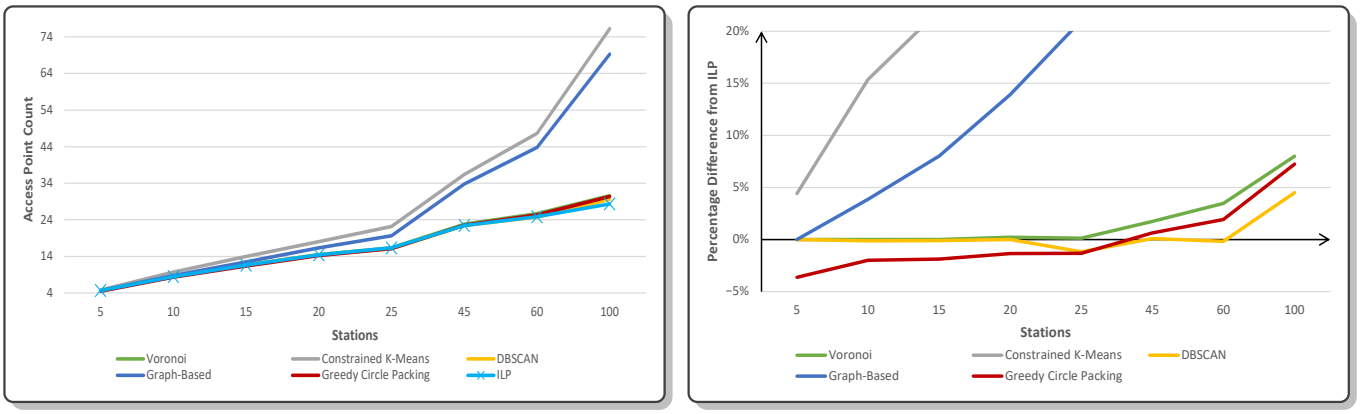

(**a**) (**b**)

Figure 9. (**a**) Number of access points created by each algorithm. (**b**) Percentage difference of AP count from ILP (X-axis).

The access point generation analysis reveals substantial differences in clustering efficiency across algorithms. ILP consistently achieves the minimum or near-minimum number of access points required for complete coverage, demonstrating its mathematical optimality for the coverage minimization objective. Constrained K-Means exhibits the poorest performance in this dimension, generating significantly more access points than necessary, particularly in larger networks where it creates 76 access points for 100 stations compared to the optimal 28 of ILP. This poor performance stems from K-Means' tendency to create uniform cluster sizes regardless of spatial sensor distribution, often subdividing naturally cohesive sensor groups. Graph-Based clustering also demonstrates suboptimal access point utilization, requiring 69 access points for the same 100-station scenario, as its focus on connectivity optimization often produces numerous small, highly connected clusters. Voronoi and the DBSCAN approaches achieve performance comparable to ILP in smaller networks but show slight degradation in larger deployments, with the DBSCAN density-based approach occasionally creating fragmented clusters in sparse regions. In other words, DBSCAN splits up sensors that should logically be served by one access point into multiple tiny clusters, each requiring its own AP, leading to inefficient access point placement.

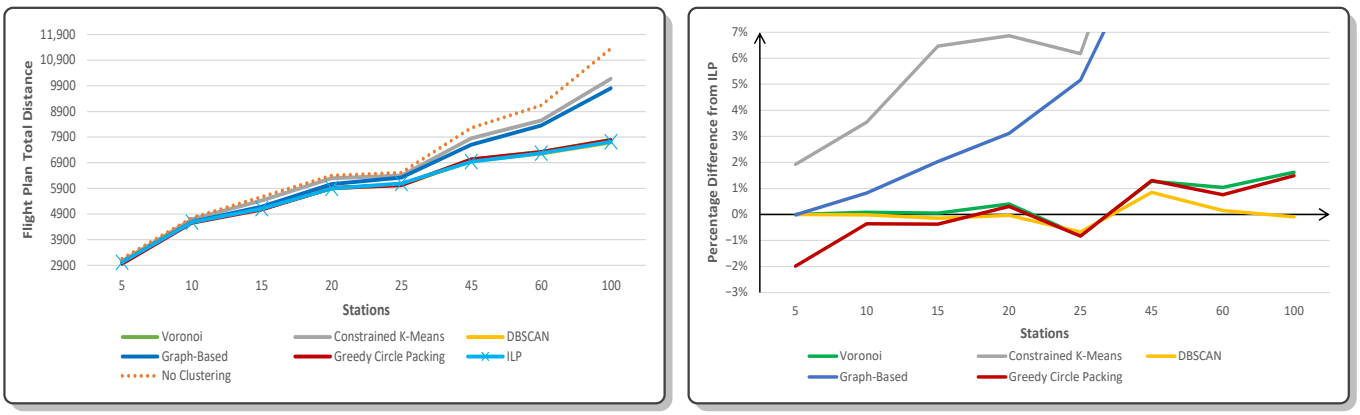

(**a**) (**b**)

Figure 10. (**a**) Total flight distance by each algorithm. (**b**) Percentage difference of flight distance from ILP (X-axis).

The flight distance analysis demonstrates the direct operational impact of access point optimization effectiveness. ILP achieves the shortest or near-shortest total flight

distances across all network configurations, with particularly pronounced advantages in large-scale deployments. For 100-station networks, ILP generates flight plans requiring 7718 distance units compared to Constrained K-Means' 10,175 units, representing a 24% improvement in travel efficiency. The baseline "No Clustering" comparison against direct sensor visitation without access point clustering reveals substantial benefits for all clustering approaches, with ILP achieving 32% distance reduction compared to the unclustered baseline of 11,354 units.

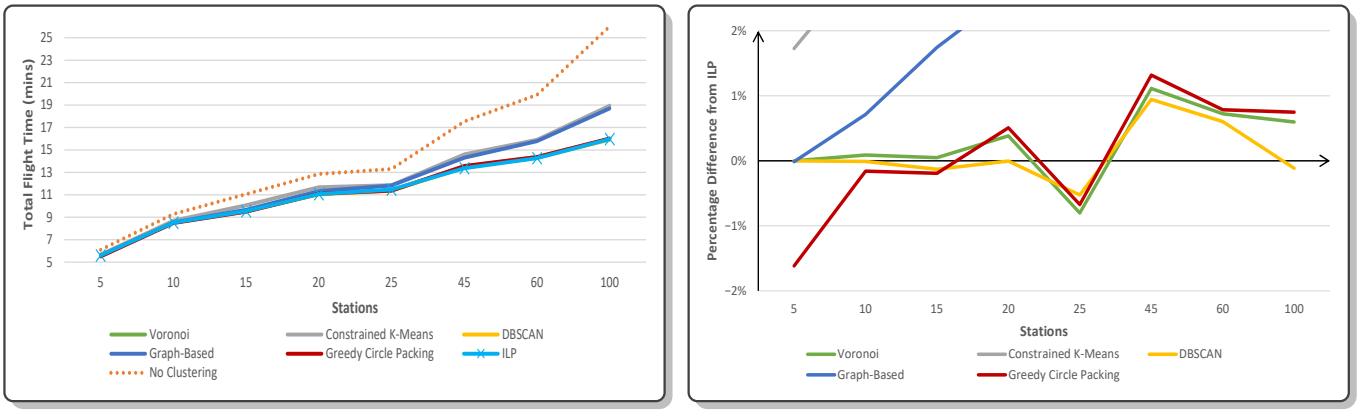

(**a**) (**b**)

Figure 11. (**a**) Total flight time (airtime) by each algorithm. (**b**) Percentage difference of flight time from ILP (X-axis).

Mission time efficiency follows similar patterns to flight distance optimization, with ILP consistently achieving the shortest or near-shortest mission durations. To calculate flight time from distances, it is assumed that a typical drone operates at a speed of 32.4 km/h, which represents typical operational velocities for commercial UAVs in data collection scenarios. The time savings become increasingly significant as network complexity grows, with ILP requiring 16 min for 100-station missions compared to Constrained K-Means' 18.9 min. Most notably, ILP demonstrates a substantial 38% improvement over the baseline "No Clustering" approach, which requires 26 min for the same 100-station deployment. These improvements translate directly into enhanced battery life utilization and increased operational range for drone-based collection systems.

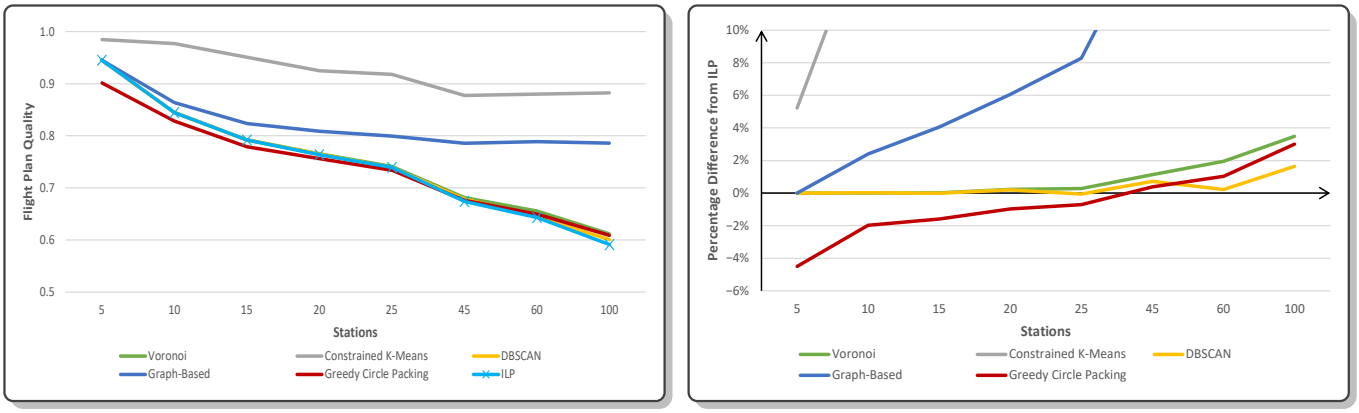

(**a**) (**b**)

Figure 12. (**a**) Flight plan quality based on the access points generated by each algorithm. (**b**) Percentage difference of quality from ILP (X-axis).

The composite quality assessment reveals the effectiveness of ILP in generating operationally efficient access point configurations. While Constrained K-Means achieves the

highest individual quality scores due to its tendency to create numerous small clusters with minimal sensor dispersion; this advantage comes at the significant cost of dramatically increased access point count and corresponding flight overhead. ILP maintains competitive quality scores while achieving superior efficiency in access point utilization, representing an optimal balance between collection efficiency and routing optimization.

Graph-Based clustering demonstrates consistently superior quality scores compared to other algorithms while maintaining reasonable access point counts, suggesting potential for hybrid approaches that combine the mathematical optimality of ILP with graph-based quality enhancement techniques. However, the increased access point count required by Graph-Based methods ultimately results in longer flight times that offset the quality advantages in practical mission scenarios.

While ILP consistently demonstrates superior performance across operational metrics, computational efficiency represents a critical consideration for real-world deployment scenarios. The mathematical optimality guarantees provided by integer linear programming come at the cost of increased computational complexity, particularly as network size grows. Figure 13 presents a comprehensive analysis of computational time requirements across all evaluated algorithms, measured in seconds for varying network configurations.

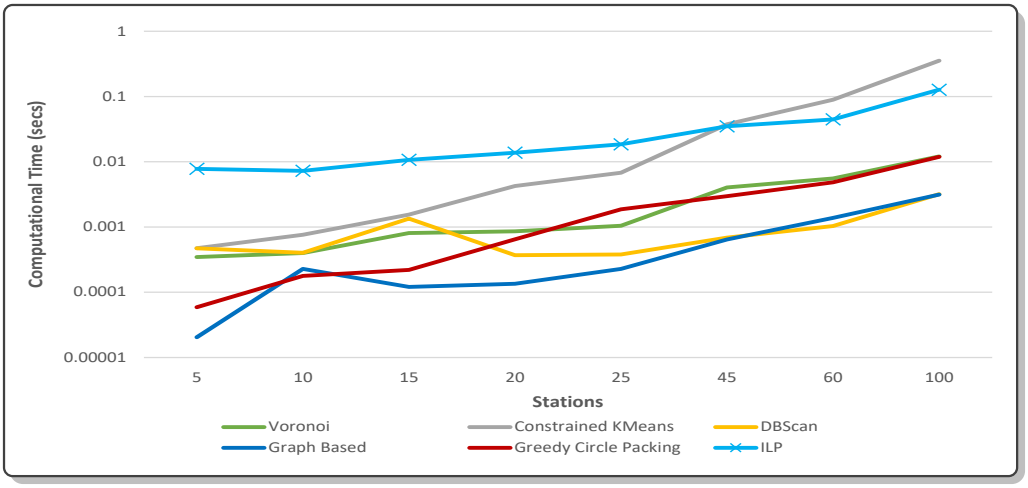

Figure 13. Computational time (runtime) comparison across clustering algorithms.

The computational analysis reveals distinct performance characteristics across algorithmic approaches. Graph-Based clustering demonstrates the most favorable computational efficiency, requiring only 0.003 s for the largest tested network. Conversely, ILP and Constrained K-Means exhibit significantly higher computational overhead, particularly in large-scale deployments. For 100-station networks, ILP requires approximately 0.127 s while Constrained K-Means demands 0.354 s. The exponential growth in computational requirements for Constrained K-Means reflects its iterative optimization process and sensitivity to initialization parameters, while the ILP computational cost grows more moderately due to its systematic constraint satisfaction approach.

Despite the higher computational cost of ILP relative to heuristic methods, several factors mitigate this limitation in practical applications. First, access point optimization represents a strategic planning phase typically executed offline rather than in real-time operational contexts. The computational investment of 0.127 s for 100-station networks yields mathematically optimal solutions that provide long-term operational benefits through minimized energy consumption and extended mission capabilities.

Second, the absolute computational times remain highly manageable for most practical deployment scenarios. Even the largest tested configuration completes optimization within

a fraction of a second, making ILP suitable for deployment planning, periodic reconfiguration, and scenario analysis applications where solution optimality justifies the modest computational overhead.

For applications requiring real-time reconfiguration or extremely large-scale networks, hybrid approaches combining fast heuristic methods for initial placement with ILP-based refinement for critical regions may provide optimal balance between computational efficiency and solution quality. The modular nature of our two-phase framework facilitates such adaptive implementations where algorithmic selection can be dynamically adjusted based on operational constraints and performance requirements. The computational efficiency analysis reinforces the practical viability of ILP while highlighting alternative approaches for time-critical applications where near-optimal solutions suffice.

4.4. Comprehensive Performance Summary

To facilitate practical algorithm selection, Table 9 consolidates the performance metrics across all evaluated approaches and network configurations. This comprehensive comparison enables practitioners to assess the trade-offs between computational efficiency, operational performance, and resource requirements based on their specific deployment constraints.

Table 9. Comprehensive performance comparison across all approaches and network configurations. Bold values indicate best performance in each category.

Stations	Metric	ILP	Voronoi	Constrained K-Means	DBSCAN	Graph-Based	Greedy Circle Packing	No Clustering
5	Distance	3016.4	3016.4	3062.1	3016.4	3016.6	**2959.4**	3159.6
	Airtime	5.6	5.6	5.7	5.6	5.6	**5.5**	6.1
	APs	**5**	5	5	5	5	4	-
	Quality	0.9	0.9	**1.0**	0.9	0.9	0.9	-
	Runtime	0.0078	0.0003	0.0005	0.0005	**0.0000**	0.0001	-
10	Distance	4579.9	4583.9	4696.6	4577.8	4598.2	**4558.8**	4746.7
	Airtime	**8.5**	8.5	8.7	8.5	8.5	8.5	9.3
	APs	**8**	8	10	8	9	8	-
	Quality	0.8	0.8	**1.0**	0.8	0.9	0.8	-
	Runtime	0.0072	0.0004	0.0008	0.0004	**0.0002**	0.0002	-
15	Distance	5109.1	5109.1	5430.5	**5102.5**	5187.8	5075.9	5567.0
	Airtime	**9.5**	9.5	10.1	9.5	9.7	9.5	11.1
	APs	12	12	14	12	12	**11**	-
	Quality	0.8	0.8	**1.0**	0.8	0.8	0.8	-
	Runtime	0.0107	0.0008	0.0016	0.0013	**0.0001**	0.0002	-
20	Distance	**5898.8**	5907.1	6296.1	5894.2	6067.3	5911.3	6397.9
	Airtime	**11.1**	11.1	11.7	11.1	11.3	11.1	12.8
	APs	**14**	14	18	14	16	14	-
	Quality	0.8	0.8	**0.9**	0.8	0.8	0.8	-
	Runtime	0.0138	0.0009	0.0043	0.0004	**0.0001**	0.0006	-
25	Distance	6085.6	6032.5	6399.9	6042.6	6323.9	**6025.9**	6511.4
	Airtime	11.5	**11.4**	11.9	11.4	11.8	11.4	13.3
	APs	**16**	16	22	16	20	16	-
	Quality	0.7	0.7	**0.9**	0.7	0.8	0.7	-
	Runtime	0.0185	0.0010	0.0068	0.0004	**0.0002**	0.0019	-
45	Distance	**6941.6**	7028.5	7850.2	6963.5	7604.3	7032.6	8254.8
	Airtime	**13.4**	13.5	14.6	13.4	14.3	13.6	17.5
	APs	**22**	23	36	22	34	23	-
	Quality	0.7	0.7	**0.9**	0.7	0.8	0.7	-
	Runtime	0.0349	0.0040	0.0374	**0.0007**	0.0006	0.0030	-

Table 9. *Cont.*

Stations	Metric	ILP	Voronoi	Constrained K-Means	DBSCAN	Graph-Based	Greedy Circle Packing	No Clustering
60	Distance	7267.0	7327.9	8544.1	**7255.3**	8354.7	7317.9	9138.1
	Airtime	**14.3**	14.3	15.9	14.3	15.8	14.4	19.9
	APs	**25**	26	48	25	44	25	-
	Quality	0.6	0.7	**0.9**	0.6	0.8	0.6	-
	Runtime	0.0446	0.0056	0.0892	**0.0010**	0.0014	0.0048	-
100	Distance	7717.9	7792.5	10174.9	**7686.5**	9807.5	7781.7	11353.8
	Airtime	16.0	16.0	18.9	**15.9**	18.7	16.0	26.0
	APs	**28**	31	76	30	69	30	-
	Quality	0.6	0.6	**0.9**	0.6	0.8	0.6	-
	Runtime	0.1271	0.0120	0.3537	0.0032	**0.0031**	0.0119	-

The consolidated results reveal several key performance patterns across the evaluated methodologies. In terms of access point efficiency, ILP demonstrates consistent optimization by achieving the minimum or near-minimum number of access points across all network sizes. This superior coverage optimization becomes particularly evident in large-scale deployments, where ILP requires only 28 access points for 100-station networks compared to Constrained K-Means' excessive requirement of 76 access points for the same configuration.

Flight performance analysis shows ILP delivering competitive distances and mission times across all tested configurations, with pronounced advantages in larger network deployments. The baseline "No Clustering" approach consistently exhibits significantly higher operational costs, validating the fundamental effectiveness of clustering-based methodologies for drone data collection optimization.

Quality assessment results indicate that while Constrained K-Means achieves the highest composite quality scores, this performance comes at the substantial cost of excessive access point proliferation. ILP maintains reasonable quality characteristics while prioritizing the primary optimization objective of minimizing collection infrastructure requirements.

Computational performance varies significantly across approaches, with Graph-Based and Voronoi methods demonstrating superior execution speed. Constrained K-Means exhibits exponential computational growth that limits its scalability for large network deployments. Despite higher computational overhead compared to heuristic approaches, the ILP execution times remain highly manageable for practical deployment scenarios, with optimization completing within fractions of a second even for the largest tested configurations.

These consolidated findings reinforce the effectiveness of ILP-based access point selection for drone data collection optimization. ILP consistently achieves the fundamental objective of minimizing access point count while maintaining competitive or superior performance across operational metrics. The mathematical optimality guarantees provided by integer linear programming ensure reliable performance across diverse network configurations, making ILP the preferred approach for mission-critical applications where efficiency and predictability are paramount.

This comprehensive evidence strengthens our foundational premise that ILP-based clustering provides the optimal foundation for the two-phase optimization strategy, effectively balancing the competing objectives of coverage minimization, routing efficiency, and operational quality in drone-based wireless sensor network data collection scenarios.

Benchmark Selection Justification

The comparative evaluation employs six established clustering algorithms that represent the primary algorithmic families used for access point placement in WSN scenarios.

Our benchmark selection was guided by several strategic considerations that ensure comprehensive and fair evaluation while addressing the unique constraints of drone-based data collection systems. These are as follows.

Algorithmic Diversity: The selected methods encompass the major categories of clustering approaches used in WSN applications. They are as follows: geometric-based clustering (Voronoi tessellation), density-based clustering (DBSCAN), centroid-based clustering (K-Means variants), constrained optimization (Constrained K-Means), graph-based methods (Graph-Based clustering), and geometric packing (Greedy Circle Packing). This diversity ensures comprehensive evaluation across different algorithmic paradigms, ranging from exact mathematical formulations to approximate heuristics designed for computational efficiency in large-scale deployments.

Metaheuristic Method Limitations: While metaheuristic approaches such as genetic algorithms, particle swarm optimization, and simulated annealing are widely used in optimization problems, they face fundamental limitations when applied to our specific problem formulation. These methods typically lack convergence guarantees and require extensive parameter tuning, making them unsuitable for mission-critical drone deployment scenarios where reliability and predictability are paramount. Moreover, metaheuristic approaches cannot provide the mathematical optimality guarantees essential for strategic access point placement decisions that influence long-term operational efficiency and mission success rates.

Absence of Comparable Hybrid Methods: Our enhanced literature review, including recent bilevel optimization approaches [7,20] and energy-efficient clustering strategies [8,9], confirms that no existing work combines ILP for access point placement with mTSP for multi-drone routing in WSN data collection scenarios. Recent metaheuristic approaches either employ heuristic algorithms rather than mathematical optimization or focus on ground-based routing without aerial coordination considerations. The bilevel optimization framework by Han et al. [7], while innovative, relies on heuristic methods (improved dandelion algorithm and iterated greedy algorithm) that lack mathematical optimality guarantees and does not address multi-drone coordination requirements inherent in large-scale WSN deployments.

Domain-Specific Constraint Considerations: The unique operational requirements of drone-based WSN data collection introduce constraints that distinguish our problem from traditional clustering scenarios. Unlike ground-based systems where cluster heads are existing network nodes, our access points represent physical locations that drones must visit and hover at for extended periods. This fundamental difference invalidates many established benchmarks from related domains, as traditional clustering algorithms lack consideration for physical coverage constraints, communication range limitations, flight energy consumption patterns, and the geometric complexities of hovering data collection missions.

Computational Optimality Requirements: The selection of exact algorithms over metaheuristic approaches reflects the strategic planning nature of access point deployment, where mathematical optimality guarantees provide significant value. Unlike real-time operational scenarios, AP placement represents a one-time strategic decision that influences long-term operational efficiency. The modest computational overhead of ILP (under 0.13 s for 100-station networks as demonstrated in Figure 13) provides mathematically optimal solutions that eliminate the uncertainty associated with metaheuristic approaches.

Standardized Problem Formulation: The selected algorithms address the identical optimization challenge—minimizing the number of collection points while ensuring complete sensor coverage. This enables fair performance evaluation where improvements

can be attributed to our methodological innovations rather than differences in problem assumptions or objectives.

Established WSN Baselines: These methods represent the state-of-the-art baselines consistently used in WSN clustering evaluation, providing standardized comparison points that contextualize our results within the broader WSN optimization literature [45–53]. The selected algorithms have been extensively validated in WSN applications and provide reliable performance benchmarks that enable meaningful comparison with our ILP-based approach.

5. Conclusions

Our research demonstrates that combining ILP and mTSP creates a powerful framework for drone-based data collection in wireless sensor networks. The two-phase approach—using ILP for strategic access point placement first, then applying mTSP for flight path optimization—offers significant advantages over single-stage methods.

Breaking complex problems into sequential stages dramatically reduces computational demands in large-scale deployments. Our tests reveal that this clustered approach not only improves scalability but also extends drone battery life through more efficient routing. The framework effectively balances energy constraints with operational requirements.

Comparative evaluation against six established clustering algorithms validates the superiority of ILP-based access point selection. While alternatives like Voronoi tessellation and Graph-Based clustering show merit in specific scenarios, ILP consistently achieves optimal access point minimization while maintaining competitive operational quality. The mathematical guarantees provided by integer linear programming ensure reliable performance across diverse network configurations.

The quality assessment framework introduced in this work provides practitioners with tools for evaluating operational effectiveness beyond simple distance metrics. Our post-processing enhancement technique addresses the inherent limitations in pure ILP formulations, showing consistent but modest improvements in composite quality scores across all tested scenarios through optimized sensor assignments.

These methodologies have broad applications beyond academic interest. Environmental monitoring programs, emergency response coordination, and commercial delivery systems can all benefit from the efficiency gains observed herein.

Future research directions might explore dynamic reconfiguration mechanisms that adapt both access point placement and flight paths in real-time. Incorporating predictive optimization through machine learning techniques could further enhance system performance.

Investigating recently developed clustering algorithms also represents a promising avenue for performance improvements. Density-center-based automatic clustering algorithms [54], which identify cluster centers based on local density peaks, may offer enhanced access point selection by naturally detecting optimal aggregation points in sensor networks. Similarly, multi-view dynamic kernelized evidential clustering approaches [55], which leverage multiple data perspectives and uncertainty modeling, could provide more robust access point configurations that account for varying operational conditions and environmental uncertainties. Integrating these advanced clustering methodologies with our ILP-based optimization framework merits future investigation.

Future work will also incorporate explicit battery constraints and detailed energy consumption models for specific drone platforms. While the current framework optimizes energy efficiency through reduced travel distances, integrating realistic energy models that account for battery capacity, power consumption during different flight phases, and environmental factors would enable more precise mission planning and optimal fleet composition.

Furthermore, the current model assumes isotropic communication within a fixed radius and perfect knowledge of sensor and drone locations, which may not hold in complex real-world environments. Future work should address two critical extensions to enhance practical applicability.

First, environments with obstacles or directional transmission limitations require obstacle-aware coverage constraints. The ILP formulation can be extended by redefining the binary variable $covers[s, ap]$ (Algorithm 1) to account for line-of-sight (LOS) [56] conditions between sensors and access points. Additionally, candidate AP locations can be preprocessed to exclude infeasible positions such as those inside obstacles or without sufficient clearance, ensuring that AP placements are both coverage-optimal and physically realizable in complex terrains.

Second, positional uncertainty from GPS inaccuracies, environmental drift, or dynamic obstacles necessitates robust optimization extensions [57]. The ILP phase could incorporate coverage constraints that ensure robustness under worst-case deviations within uncertainty bounds for sensor and AP positions. Alternatively, stochastic programming approaches could model uncertain parameters via probability distributions to maximize expected coverage or minimize coverage failure risk. Similarly, the mTSP phase could optimize drone routes to remain feasible under location uncertainties by incorporating buffer zones or robust tour constraints.

These extensions will enhance the framework's applicability in uncertain and obstructed environments while maintaining the fundamental advantages of the two-phase optimization approach.

With Internet of Things ecosystems rapidly expanding, these sophisticated optimization approaches will become increasingly vital for building sustainable data collection infrastructures capable of addressing future challenges.

Author Contributions: Conceptualization, G.G. and I.K.; methodology, G.G. and I.K.; software, G.G. and I.K.; validation, G.G. and I.K.; formal analysis, G.G. and I.K.; investigation, G.G. and I.K.; resources, G.G. and I.K.; data curation, G.G. and I.K.; writing—original draft preparation, G.G. and I.K.; writing—review and editing, G.G. and I.K.; visualization, G.G. and I.K.; supervision, I.K.; project administration, I.K. All authors have read and agreed to the published version of the manuscript.

Funding: This research received no external funding.

Institutional Review Board Statement: Not applicable.

Informed Consent Statement: Not applicable.

Data Availability Statement: The original data presented in the study are openly available in "ILP and mTSP Integration" GitHub repository at: https://github.com/ggasteratos/ILP-and-mTSP-Integration (accessed on 1 September 2025) in Microsoft Excel (version 2507) format.

Conflicts of Interest: The authors declare no conflicts of interest.

References

1. Onuekwusi, N.; Okpara, C. Wireless sensor networks (WSN): An overview. *Am. Sci. Res. J. Eng. Technol. Sci.* **2020**, *64*, 53–63.
2. Wang, J.; Wang, N.; Wang, H.; Cao, K.; El-Sherbeeny, A.M. GCP: A multi-strategy improved wireless sensor network model for environmental monitoring. *Comput. Netw.* **2024**, *254*, 110807. https://doi.org/10.1016/j.comnet.2024.110807.
3. Križanović, V.; Grgić, K.; Spišić, J.; Žagar, D. An advanced energy-efficient environmental monitoring in precision agriculture using LoRa-based wireless sensor networks. *Sensors* **2023**, *23*, 6332. https://doi.org/10.3390/s23146332.
4. Chen, D.; Zhang, Y.; Pang, G.; Gao, F.; Duan, L. A hybrid scheme for disaster-monitoring applications in wireless sensor networks. *Sensors* **2023**, *23*, 5068. https://doi.org/10.3390/s23115068.
5. Balbal, S.; Bouamama, S.; Blum, C. A Greedy Heuristic for Maximizing the Lifetime of Wireless Sensor Networks Based on Disjoint Weighted Dominating Sets. *Algorithms* **2021**, *14*, 170. https://doi.org/10.3390/a14060170.

6. Laporte, G. The traveling salesman problem: An overview of exact and approximate algorithms. *Eur. J. Oper. Res.* **1992**, *59*, 231–247. https://doi.org/10.1016/0377-2217(92)90138-Y.
7. Han, S.; Zhu, K.; Zhou, M.; Liu, X. Joint Deployment Optimization and Flight Trajectory Planning for UAV Assisted IoT Data Collection: A Bilevel Optimization Approach. *IEEE Trans. Intell. Transp. Syst.* **2022**, *23*, 21492–21504. https://doi.org/10.1109/TITS.2022.3180288.
8. Tan, N.D.; Le, T.T.H. Machine learning-based IoT: Developing an energy-efficient and balanced clustering routing protocol (EEB-CR) for WSNs. *J. Netw. Comput. Appl.* **2025**, *242*, 104269. https://doi.org/10.1016/j.jnca.2025.104269.
9. Liang, Y.; Zhao, S.; Liu, X.; He, H.; Zhao, X.; Wang, H. A Balanced Energy-Efficient Clustering Strategy for WSNs. *IEEE Sens. J.* **2024**, *24*, 38035–38044. https://doi.org/10.1109/JSEN.2024.3458425.
10. Karunanithy, K.; Velusamy, B.; Krishnakumar, S.; Senthilkumar, V.J. Energy-Efficient Data Routing in Landslide-Prone Area Using Wireless Sensor Networks With Drone. *IEEE Internet Things J.* **2024**, *11*, 4497–4507. https://doi.org/10.1109/JIOT.2023.3301955.
11. Gasteratos, G.; Karydis, I. Optimized Drone Data Collection in WSNs: An ILP and mTSP Framework. *Appear Int. J. Inform. Vis.* **2025**, *9*.
12. Jünger, M.; Liebling, T.; Naddef, D.; Nemhauser, G.; Pulleyblank, W.; Reinelt, G.; Rinaldi, G.; Wolsey, L. *50 Years of Integer Programming 1958–2008. From the Early Years to the State-of-the-Art. Papers Based on the Presentations at the Special Session at the 12th Combinatorial Optimization Workshop AUSSOIS 2008, Aussois, France, 7–11 January 2008. With DVD*; Springer: Berlin/Heidelberg, Germany, 2010. https://doi.org/10.1007/978-3-540-68279-0.
13. Bektaş, T. The multiple traveling salesman problem: An overview of formulations and solution procedures. *Omega-Int. J. Manag. Sci.* **2006**, *34*, 209–219. https://doi.org/10.1016/J.OMEGA.2004.10.004.
14. Cheikhrouhou, O.; Khoufi, I. A comprehensive survey on the Multiple Traveling Salesman Problem: Applications, approaches and taxonomy. *Comput. Sci. Rev.* **2021**, *40*, 100369. https://doi.org/10.1016/j.cosrev.2021.100369.
15. Aouedi, O.; Vu, T.H.; Sacco, A.; Nguyen, D.C.; Piamrat, K.; Marchetto, G.; Pham, Q.V. A Survey on Intelligent Internet of Things: Applications, Security, Privacy, and Future Directions. *IEEE Commun. Surv. Tutor.* **2024**, *27*, 1238–1292. https://doi.org/10.1109/COMST.2024.3430368.
16. Nguyen, M.T.; Nguyen, C.V.; Do, H.T.; Hua, H.T.; Tran, T.A.; Nguyen, A.D.; Ala, G.; Viola, F. Uav-assisted data collection in wireless sensor networks: A comprehensive survey. *Electronics* **2021**, *10*, 2603. https://doi.org/10.3390/electronics10212603.
17. Shah, R.; Roy, S.; Jain, S.; Brunette, W. Data MULEs: Modeling and analysis of a three-tier architecture for sparse sensor networks. *Ad Hoc Netw.* **2003**, *1*, 215–233. https://doi.org/10.1016/S1570-8705(03)00003-9.
18. Gatzianas, M.; Georgiadis, L. A Distributed Algorithm for Maximum Lifetime Routing in Sensor Networks with Mobile Sink. *IEEE Trans. Wirel. Commun.* **2008**, *7*, 984–994. https://doi.org/10.1109/TWC.2008.060727.
19. Chakrabarti, A.; Sabharwal, A.; Aazhang, B. Using Predictable Observer Mobility for Power Efficient Design of Sensor Networks. In *Information Processing in Sensor Networks*; Zhao, F., Guibas, L., Eds.; Springer: Berlin/Heidelberg, Germany, 2003; pp. 129–145. https://doi.org/10.1007/3-540-36978-3{_}9.
20. Han, S.; Liu, X.; Zhou, M.; Zhu, K.; Zhao, L.; Albeshri, A.; Abusorrah, A. Joint Association, Deployment and Flight Trajectory Optimization for Multi-UAV-Enabled Large-Scale Mobile Edge Computing. *IEEE Trans. Mob. Comput.* **2024**, *23*, 13207–13221. https://doi.org/10.1109/TMC.2024.3426945.
21. Heinzelman, W.; Chandrakasan, A.; Balakrishnan, H. Energy-efficient communication protocol for wireless microsensor networks. In Proceedings of the 33rd Annual Hawaii International Conference on System Sciences, Maui, HI, USA, 7 January 2000; Volume 2, p. 10. https://doi.org/10.1109/HICSS.2000.926982.
22. Younis, O.; Fahmy, S. HEED: A hybrid, energy-efficient, distributed clustering approach for ad hoc sensor networks. *IEEE Trans. Mob. Comput.* **2004**, *3*, 366–379. https://doi.org/10.1109/TMC.2004.41.
23. Gupta, G.; Younis, M. Fault-tolerant clustering of wireless sensor networks. In Proceedings of the 2003 IEEE Wireless Communications and Networking (WCNC 2003), New Orleans, LA, USA, 16–20 March 2003; Volume 3, pp. 1579–1584. https://doi.org/10.1109/WCNC.2003.1200622.
24. Gandham, S.; Dawande, M.; Prakash, R.; Venkatesan, S. Energy efficient schemes for wireless sensor networks with multiple mobile base stations. In Proceedings of the GLOBECOM'03. IEEE Global Telecommunications Conference (IEEE Cat. No.03CH37489), San Francisco, CA, USA, 1–5 December 2003; Volume 1, pp. 377–381. https://doi.org/10.1109/GLOCOM.2003.1258265.
25. Roberti, R.; Ruthmair, M. Exact Methods for the Traveling Salesman Problem with Drone. *Transp. Sci.* **2021**, *55*, 315–335. https://doi.org/10.1287/trsc.2020.1017.
26. Zhou, H.; Qin, H.; Cheng, C.; Rousseau, L.M. An exact algorithm for the two-echelon vehicle routing problem with drones. *Transp. Res. Part B Methodol.* **2023**, *168*, 124–150. https://doi.org/10.1016/j.trb.2023.01.002.
27. Meskar, M.; Ahmadi-Javid, A. Optimizing Drone Delivery Paths from Shared Bases: A Location-Routing Problem with Realistic Energy Constraints. *J. Intell. Robot. Syst.* **2024**, *110*, 142. https://doi.org/10.1007/s10846-024-02129-9.
28. Li, X.; Zhu, L.; Chu, X.; Fu, H. Edge computing-enabled wireless sensor networks for multiple data collection tasks in smart agriculture. *J. Sens.* **2020**, *2020*, 4398061. https://doi.org/10.1155/2020/4398061.

29. Castaño, F.; Rossi, A.; Sevaux, M.; Velasco, N. A column generation approach to extend lifetime in wireless sensor networks with coverage and connectivity constraints. *Comput. Oper. Res.* **2014**, *52*, 220–230. https://doi.org/10.1016/j.cor.2013.11.001.
30. Gu, Y.; Zhao, B.H.; Ji, Y.S.; Li, J. Theoretical Treatment of Target Coverage in Wireless Sensor Networks. *J. Comput. Sci. Technol.* **2011**, *26*, 117–129. https://doi.org/10.1007/s11390-011-9419-4.
31. Cornejo-Acosta, J.A.; García-Díaz, J.; Pérez-Sansalvador, J.C.; Segura, C. Compact Integer Programs for Depot-Free Multiple Traveling Salesperson Problems. *Mathematics* **2023**, *11*, 3014. https://doi.org/10.3390/math11133014.
32. Kumar, S.; Munapo, E.; Philimon, N. An Insight into the Characteristic Equation for an Integer Program. *Int. J. Math. Eng. Manag. Sci.* **2021**, *6*, 611–620. https://doi.org/10.33889/IJMEMS.2021.6.2.037.
33. Benghelima, S.C.; Ould-Khaoua, M.; Benzerbadj, A.; Baala, O. Multi-objective Optimisation of Wireless Sensor Networks Deployment: Application to fire surveillance in smart car parks. In Proceedings of the 2021 International Wireless Communications and Mobile Computing (IWCMC), Harbin, China, 28 June–2 July 2021; pp. 98–104. https://doi.org/10.1109/IWCMC51323.2021.9498747.
34. Mohamed, M.D.S.; Patrick, F.; Ohta, C. LPCHS: Linear programming based cluster head selection method in wireless sensor networks. *IEICE Commun. Express* **2023**, *12*, 511–516. https://doi.org/10.1587/comex.2023XBL0073.
35. Fellah, S.; Kaddour, M. Exact and efficient heuristic deployment in WSN under coverage, connectivity, and lifetime constraints. In *Sensor Technology: Concepts, Methodologies, Tools, and Applications*; IGI Global: Hershey, PA, USA, 2020; pp. 1082–1099. https://doi.org/10.4018/978-1-7998-2454-1.ch051.
36. Kara, I.; Bektas, T. Integer linear programming formulations of multiple salesman problems and its variations. *Eur. J. Oper. Res.* **2006**, *174*, 1449–1458. https://doi.org/10.1016/j.ejor.2005.03.008.
37. Wang, C.; Ma, F.; Yan, J.; De, D.; Das, S.K. Efficient Aerial Data Collection with UAV in Large-Scale Wireless Sensor Networks. *Int. J. Distrib. Sens. Netw.* **2015**, *11*, 286080. https://doi.org/10.1155/2015/286080.
38. Wikipedia Contributors. Inverse-Square Law. 2025. Available online: https://en.wikipedia.org/wiki/Inverse-square_law (accessed on 29 July 2025).
39. Bhadra, D.R.; Joshi, C.A.; Soni, P.R.; Vyas, N.P.; Jhaveri, R.H. Packet loss probability in wireless networks: A survey. In Proceedings of the 2015 International Conference on Communications and Signal Processing (ICCSP), Melmaruvathur, India, 2015, pp. 1348–1354. https://doi.org/10.1109/ICCSP.2015.7322729.
40. Bada, A. Automatic Repeat Request (Arq) Protocols. The International Journal of Engineering and Science (IJES) **2017**, 6, pp. 64–66. https://www.researchgate.net/publication/359440514
41. Gasteratos, G.; Karydis, I. Path Planning Optimisation for Multiple Drones: Repositioning the Starting Point. In Proceedings of the IFIP International Conference on Artificial Intelligence Applications and Innovations, Corfu, Greece, 27–30 June 2024; Springer: Berlin/Heidelberg, Germany, 2024; pp. 211–223. https://doi.org/10.1007/978-3-031-63223-5_16.
42. Gasteratos, G.; Karydis, I. Efficient Drone Path Planning through Strategic Launch Pad Positioning. In Proceedings of the 1st International Conference on Drones and Unmanned Systems (DAUS'2025), Granada, Spain, 19–21 February 2025; IFSA Publishing: Castelldefels, Spain , 2025; pp. 254–259. https://doi.org/10.13140/RG.2.2.18747.94240.
43. Google Or-Tools. 2025. Available online: https://developers.google.com/optimization (accessed on 24 March 2025).
44. Bernard, R.; Robert, J.G.; Mei-Ling, T.L. The Wilcoxon signed rank test for paired comparisons of clustered data. *Biometrics* **2006**, *62*, 185–192. https://doi.org/10.1111/j.1541-0420.2005.00389.x.
45. Aurenhammer, F. Voronoi diagrams—A survey of a fundamental geometric data structure. *ACM Comput. Surv.* **1991**, *23*, 345–405. https://doi.org/10.1145/116873.116880.
46. Okabe, A.; Boots, B.; Sugihara, K.; Chiu, S.N. *Spatial Tessellations: Concepts and Applications of Voronoi Diagrams*; John Wiley & Sons: Hoboken, NJ, USA, 2000.
47. Bradley, P.S.; Bennett, K.P.; Demiriz, A. *Constrained k-Means Clustering*; Technical Report MSR-TR-2000-65, Microsoft Research; 2000.
48. Wagstaff, K.; Cardie, C.; Rogers, S.; Schrödl, S. Constrained K-means Clustering with Background Knowledge. In Proceedings of the Eighteenth International Conference on Machine Learning (ICML'01), San Francisco, CA, USA, 28 June–1 July 2001; pp. 577–584.
49. Ester, M.; Kriegel, H.P.; Sander, J.; Xu, X. A Density-Based Algorithm for Discovering Clusters in Large Spatial Databases with Noise. In Proceedings of the 2nd International Conference on Knowledge Discovery and Data Mining (KDD-96), Portland, OR, USA, 2–4 August 1996; AAAI Press: Washington, DC, USA , 1996; pp. 226–231.
50. Schubert, E.; Sander, J.; Ester, M.; Kriegel, H.P.; Xu, X. DBSCAN revisited, revisited: Why and how you should (still) use DBSCAN. *ACM Trans. Database Syst. (TODS)* **2017**, *42*, 19. https://doi.org/10.1145/3068335.
51. Schaeffer, S.E. Graph clustering. *Comput. Sci. Rev.* **2007**, *1*, 27–64. https://doi.org/10.1016/j.cosrev.2007.05.001.
52. Chen, M.; Tang, X.; Song, T.; Zeng, Z.; Peng, X.; Liu, S. Greedy heuristic algorithm for packing equal circles into a circular container. *Comput. Ind. Eng.* **2018**, *119*, 114–120. https://doi.org/https://doi.org/10.1016/j.cie.2018.03.030.

53. Hifi, M.; M'Hallah, R. A literature review on circle and sphere packing problems: Models and methodologies. *Adv. Oper. Res.* **2009**, *2009*, 150624 . https://doi.org/10.1155/2009/150624.
54. Zhang, T.; Zhou, M.; Guo, X.; Qi, L.; Abusorrah, A. A Density-Center-Based Automatic Clustering Algorithm for IoT Data Analysis. *IEEE Internet Things J.* **2022**, *9*, 24682–24694. https://doi.org/10.1109/JIOT.2022.3194886.
55. Xu, J.; Zhang, Z.; Lin, Z.; Chen, Y.; Ding, W. Multi-View Dynamic Kernelized Evidential Clustering. *IEEE/CAA J. Autom. Sin.* **2024**, *11*, 2435–2450. https://doi.org/10.1109/JAS.2024.124608.
56. Lyu, J.; Zeng, Y.; Zhang, R.; Lim, T.J. Placement optimization of UAV-mounted mobile base stations. *IEEE Commun. Lett.* **2017**, *21*, 604–607. https://doi.org/10.1109/LCOMM.2016.2633248.
57. Ben-Tal, A.; El Ghaoui, L.; Nemirovski, A. *Robust Optimization*; Princeton University Press: Princeton, NJ, USA, 2009; Volume 28. https://doi.org/10.1515/9781400831050.